Review

doi.org/10.1002/tcr.202400114
tcr.wiley-vch.de

THE CHEMICAL RECORD

Fundamental and Practical Aspects of Break-In/Conditioning of Proton Exchange Membrane Fuel Cells

Mitja Kostelec,[a, b] Matija Gatalo,*[a, c] and Nejc Hodnik*[a, b]

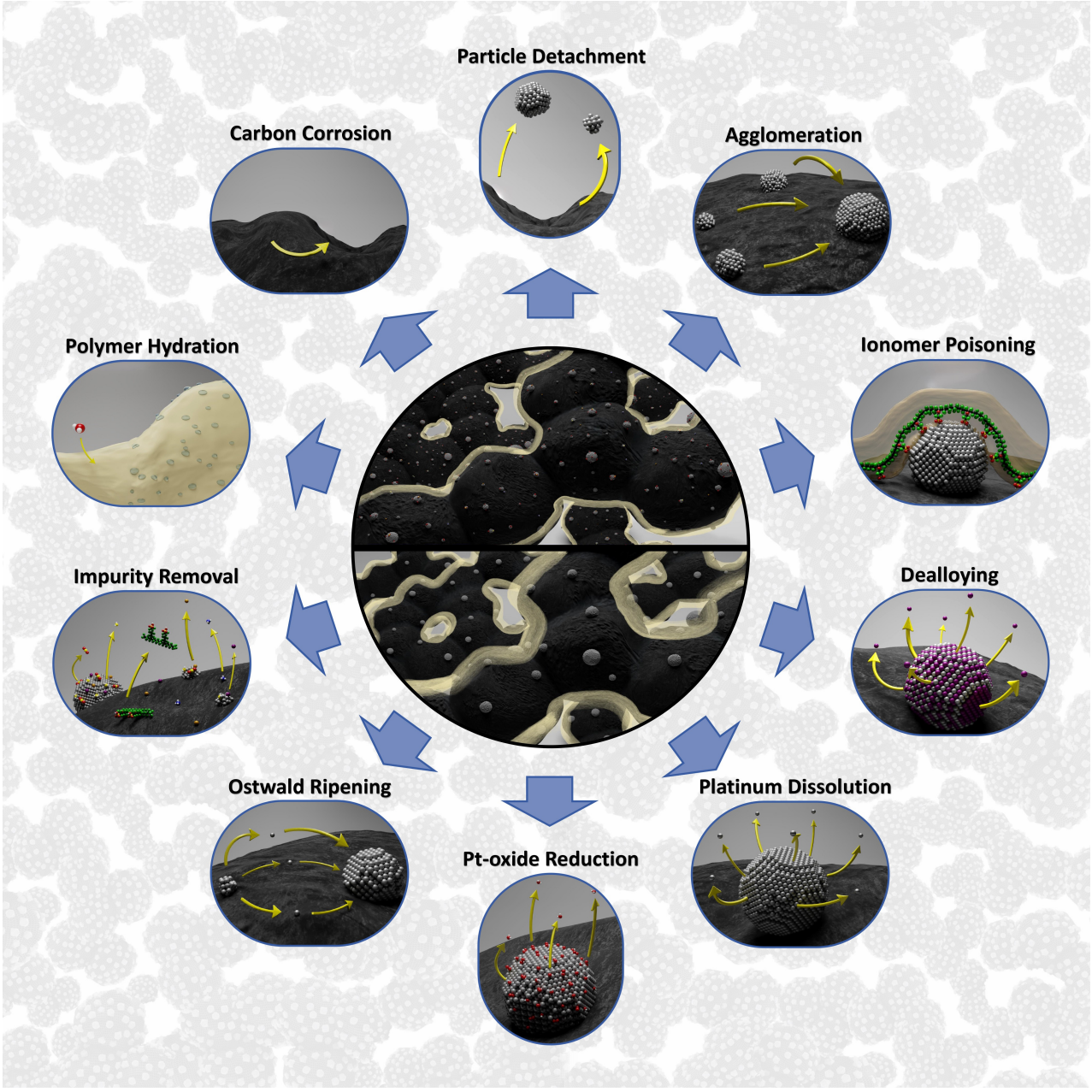

Abstract: Proton exchange membrane fuel cells (PEMFCs) have proven to be a promising power source for various applications ranging from portable devices to automotive and stationary power systems. The production of PEMFC involves numerous stages in the value chain, with each stage presenting unique challenges and opportunities to improve the overall performance and durability of the PEMFC stack. These include steps such as manufacturing the key components such as the platinum-based catalyst, processing these components into the membrane electrode assemblies (MEAs), and stacking the MEAs to ultimately produce a PEMFC stack. However, it is also known that the break-in or conditioning phase of the stack plays a crucial role in the final performance as well as durability. It involves several key phenomena such as hydration of the membrane, swelling of the ionomer, redistribution of the catalyst and the creation of suitable electrochemical interfaces – establishment of the triple phase boundary. These improve the proton conductivity, the mass transport of reactants and products, the catalytic activity of the electrode and thus the overall efficiency of the FC. The cruciality of break-in is demonstrated by the improvement in performance, which can even be over 50 % compared to the initial state. The state-of-the-art approach for the break-in of MEAs involves an electrochemical protocol, such as voltage cycling, using a PEMFC testing station. This method is time-consuming, equipment-intensive, and costly. Therefore, new, elegant, and cost-effective solutions are needed. Nevertheless, the primary aim is to achieve maximum/optimal performance so that it is fully operational and ready for the market. It is therefore essential to better understand and deconvolute these complex mechanisms taking place during break-in/conditioning. Strategies include controlled humidity and temperature cycling, novel electrode materials and other advanced break-in methods such as air braking, vacuum activation or steaming. In addition, it is critical to address the challenges associated with standardisation and quantification of protocols to enable interlaboratory comparisons to further advance the field.

Keywords: Proton exchange membrane fuel cell (PEMFC), Activation, Break-in, Conditioning, membrane electrode assembly (MEA)

1. Introduction

Proton exchange membrane fuel cells (PEMFCs) are a cutting-edge technology that enables efficient and clean energy conversion that can be used in various sectors, including portable devices, stationary power sources and various modes of transport.[1–4] They offer a promising solution for long-range and heavy-duty vehicles such as commercial trucks, buses, pickups and SUVs due to their high efficiency, scalable power, and impressive energy density.[5–6] However, despite their potential, the widespread commercialisation of PEMFCs faces significant hurdles, including challenges related to cost, durability and reliability.[7] To reach their full potential, the critical factors that determine the performance of PEMFC must be precisely optimised.

In optimisation considerations, one of the relevant processes that significantly impacts the performance and durability of PEMFC stacks is the break-in.[8–9] It is an essential part of PEMFC production as it maximises performance, and the improvement compared to the initial state can even be over 50 %.[10] In the literature, this step is also known by various terms such as conditioning, activation, commissioning or incubation.[11] In this context, a consensus on terminology is required, as activation, for example, usually refers to the production step of the electrocatalyst.[12] While the break-in process, which takes place after stack assembly and hot pressing, marks the final stage of PEMFC stack production.[8] The main objective of this process is to improve and also stabilise the performance of the PEMFC stack.[13] By creating a stable three-phase electrochemical interface and thus reducing diffusion barriers, contact resistance and ensuring long-term stability, the break-in process plays a crucial role in ensuring the optimal functionality of the entire FC system.[13]

One of the reasons why the use of PEMFCs is still not widespread is their high cost,[14–16] which is slowly starting to decrease as manufacturing improves (Figure 1).[17] While the most expensive single component of the PEMFC stack is the platinum-based catalyst (Figure 1),[14,16,18] the "break-in" phase

[a] *M. Kostelec, M. Gatalo, N. Hodnik*
Department of Materials Chemistry, National Institute of Chemistry, Hajdrihova ulica 19, 1001 Ljubljana, Slovenia
E-mail: matija.gatalo@ki.si
nejc.hodnik@ki.si
[b] *M. Kostelec, N. Hodnik*
University of Nova Gorica, Vipavska 13, SI-5000 Nova Gorica, Slovenia
[c] *M. Gatalo*
ReCatalyst d.o.o., Hajdrihova ulica 19, 1001 Ljubljana, Slovenia

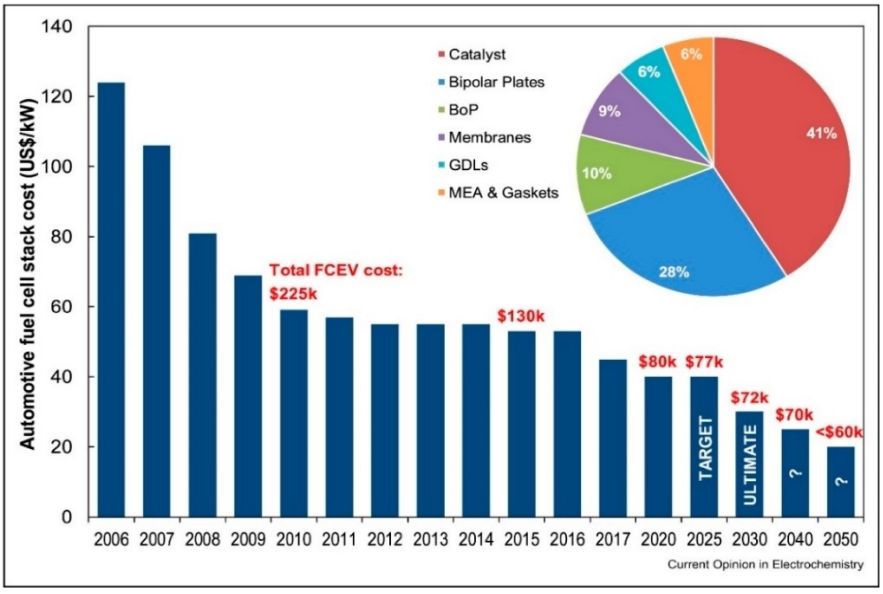

Figure 1. Evolution of automotive fuel cell cost and projection. Distribution of cost by components in pie chart. Reposted from [14], distributed under a Creative Commons Attribution License (CC BY).

stands out as the most expensive and time-consuming process in the assembly line.[11] Therefore, by optimising or shortening the break-in process, we can not only speed up production, but also reduce production costs, such as energy and material consumption, and thus, the cost of the product.[19]

It is important to note that conditioning under low stress conditions results in higher performance than under potentially faster high stress conditions. However, it is also true that conditioning under low stress conditions requires long duration, e. g. 24 h, to achieve the desired performance,[20] so it is crucial in process optimisation not to focus solely on accelerating break-in. Instead, a balanced approach should be taken, considering both the increase in performance and the time required for break-in to ensure the overall effectiveness and efficiency of the process. If we find the right balance, we can achieve the desired results while maintaining product quality and cost efficiency.

Year after year, FC technology is gaining attention, as evidenced by numerous articles,[4,21–22] company pledges[23–24] and ambitious projects.[25–27] In recent years, interest in the topic of PEMFC break-in has increased, as evidenced by the number of review articles, e. g. Yuan et al. (2011),[28] Christmann et al. (2021),[29] Kocha et al. (2022),[30] Pei et al. (2022),[31] Linden et al. (2023),[11] Ma et al. (2024).[32] Interestingly, as this is a highly interesting topic for industry and commercialisation, it has led to a decrease in the number of published research papers due to restricted disclosure. However, while some of the aforementioned reviews contain a lot of interesting features, there are also a number of misleading, poorly interpreted or even simply incorrect statements. On the other hand, research articles show correlations between the variation of parameters and their effects on the performance of PEMFC, but mostly lack a deeper understanding or even contain wrong explanations for what is happening inside the stack. Accordingly, the current state of the theory is rather inconclusive, or rather, there is no consensus on which are dominant processes take place during break-in. Therefore, an understanding of the existing literature on the conditioning of PEMFC stacks is essential to assess the current understanding of this process, identify knowledge gaps and research needs, and provide guidelines for optimising the operation of PEMFC stacks. In this review, we summarise the key findings, challenges and opportunities related to the break-in process of PEMFC stacks, focusing on the effects of various parameters such as cycling window, number of cycles, temperature (T), relative humidity (RH), pressure (p), current density and gas composition on performance and durability of PEMFCs. We will also discuss the mechanisms and models that have been proposed to explain the observed phenomena during the break-in process.[33]

1.1. Break-In or Conditioning Phase of a PEMFC

PEMFCs are electrochemical devices that convert hydrogen (H_2) and oxygen (O_2) into electricity and water. During the manufacturing process, PEMFC stacks are assembled from individual cells consisting of various components, such as the membrane electrode assembly (MEA), bipolar plates, gas

diffusion layers (GDL) and flow fields. In order to optimise the performance and durability of a PEMFC stack, it is necessary to "break-in" or "condition" it before commissioning. During break-in, the PEMFC stack is exposed to a series of controlled operating conditions (T, RH, current density etc.) to remove impurities, wet the membrane and activate the catalysts.[33–34] The aim of break-in is to improve the performance and durability of the PEMFC stack by reducing the initial degradation rate (uneven current distribution and localised overheating) and increasing the output power.[7] This is mainly done by forming/activating a triple-phase boundary (TPB) and lowering resistances, which is achieved by activating the catalyst layer (CL) – redistributing the catalyst particles and removing surface oxides (PtOx, PtOH), increasing porosity and reducing tortuosity channels, removing impurities and ensuring the passage of protons (H^+), especially by hydrating the membrane and ionomer[11,35] Various approaches to conditioning a PEMFC stack have been reported[35–36] - but the biggest common denominator of all is the very long time required for the process. Usually, the break-in takes at least several hours, but even up to several days, depending on the specific design of the PEMFC stack.

Break-in methods, and there is no universally optimal choice. It depends on many different factors, such as the membrane, the ionomer or catalyst material, the catalyst loading, the thickness of the membrane, etc.[37–38] Some methods, such as ex-situ soaking in deionised water (DI), are more aimed at conditioning the membrane and reducing its contact resistance with the catalyst,[35,39] while others, such as voltage cycling, are more suitable for activating the catalyst surface.[40] Some methods are also more suitable for certain types of membranes or electrode materials.[41–43] Therefore, the selection of a break-in method for PEMFC requires careful consideration of the critical issues (membrane, catalyst and ionomer),[44–45] as well as a thorough understanding of the advantages and disadvantages of each method. While the critical factors are improved with the break-in process, it is possible that some of them can be solved beforehand, or rather, before the PEMFC stack is assembled. Accordingly, we categorise them into two groups of methods: *In-situ* methods or so-called "electrochemical" methods, which are more suitable for laboratory scale and diagnostics, and *ex-situ* methods or "chemical-physical" methods, which are more easily transferred to mass production.[11,46]

2. Fundamental Understanding of the PEMFC Break-In

While PEMFC stacks require a break-in phase to achieve optimum performance, electrocatalyst powders are normally already subjected to an 'activation process'. Similar to the *in-situ* break-in methods for PEMFC stacks, a rather ideal way of electrocatalyst activation is based on *in-situ* electrochemical methods, e.g. using the thin-film rotating disc electrode (TF-RDE) method.[12,47–48] However, such electrochemical methods are usually only suitable for the activation of very small amounts (in the µg range) of electrocatalysts in a relatively large volume of electrolyte (few 100 mL), which is also only acceptable for academic studies and not for the actual production of electrocatalysts.[12] Consequently, the processing of large amounts of electrocatalyst powders is carried out *ex-situ* or "chemically", e.g. using acid-leach protocols in order to remove the impurities from the catalyst surface. These pre-assembly conditioning techniques aim to optimise the performance and durability of individual components.[12]

Similarly, the break-in process can be carried out using various methods, most of which are mainly suitable for research, but not necessarily for large-scale production of PEMFC stacks. For example, the conditioning of PEMFC can be performed online by integrating it into the activation bench, also called conditioning station, test station or break-in station,[11,30] and carefully regulating the voltage, current and operating parameters. With such an approach, the break-in can be monitored and adjusted in real time.[40]

However such break-in is mainly performed by online current cycling and it is thus not the most optimal method for industrial use, as it requires a costly activation bench time and is too time-consuming.[49] Therefore, alternative strategies need to be developed that would accelerate the PEMFC production line. To achieve the next generation of break-in techniques, the basic mechanisms/critical points during break-in need to be untangled.

PEMFC has an asymmetric partitioning with respect to the electrodes. The anodic reaction (hydrogen oxidation reaction, abbr. HOR) has a much higher reaction rate than the cathodic reaction (oxygen reduction reaction, abbr. ORR). Accordingly, the studies mainly focus on the improvement of the cathode, as it is the so-called bottleneck for the overall efficiency of the PEMFC.[50] In the following, we will also mainly focus on the cathode side of the PEMFC.

$$\text{Anode reaction}: \quad H_2 \rightarrow 2H^+ + 2e^- \tag{1}$$

$$\text{Cathode reaction}: \quad O_2 + 4e^- + 4H^+ \rightarrow 2H_2O \tag{2}$$

$$\text{Overall cell reaction}: \quad 2H_2 + O_2 \rightarrow 2H_2O \tag{3}$$

2.1. Triple phase Boundary

The TPB plays a central role as an interface between three indispensable phases: the catalyst, the electrolyte and the gaseous reactant.[52–53] The catalyst, which is usually made of

platinum (Pt) or precious metal alloys blended with less noble metals, acts as a promotor of the electrochemical reactions that take place in the PEMFC.[54] The electrolyte, usually a proton-conducting polymer membrane (PEM), enables the transport of H^+ between the anode and the cathode. The gaseous reactant, typically H_2, enters the anode and undergoes a catalytic reaction in which H^+ and electrons are generated. These species then combine with O_2 at the cathode and form water.[52,55]

In order to establish TPB, firstly, catalytic reactions must take place at the electrochemically active sites provided by the catalyst surface. Secondly, the presence of a wetted ionomer as an ion conductor is crucial for facilitating ion transport. However, the ionomer layer can also impede the path of the gaseous reactant to the reaction site on the catalyst. Finally, electron conduction is achieved by the catalyst itself, which consists of metal nanoparticles supported by conductive carbon. By establishing the TPB, the PEMFC fulfils the requirements for the catalytic reactions to take place on the catalyst surface, which is supported by the presence of an ionically conductive and wetted ionomer. In addition, it enables the transport of the gaseous reactant to the reaction site and facilitates electron conduction through the metal nanoparticles of the catalyst and the conductive carbon support material.[52,56]

Figure 2 a) & b) illustrate the common misconception of the TPB in the literature. It suggests that the TPB, or the site of the ORR, exists only at a singular point where all three phases intersect, which is an inaccurate interpretation. At the nanoscale, there is no definitive answer; the reaction can still occur even if the three key pathways are not in direct contact, while the resistances to bridge this gap are sufficiently low for the reactant to reach the reaction site (Figure 2c). The relative impacts of these resistances are depicted in the pie chart in Figure 2d.

Several factors influence TPB density and accessibility, such as catalyst loading, the catalyst particle size and CL structure.[59,60] For example, the catalyst particles are often supported on high surface area materials to improve their contact with the electrolyte and gaseous reactant. Thin and porous layers with a well-distributed catalyst structure can also promote the formation of TPBs, as they maximise the active surface area and facilitate the diffusion of the gaseous reactant. It is also crucial to choose suitable support materials with high conductivity and good compatibility with the electrolyte, e. g. carbon black and carbon nanotubes, which provide a larger surface area for the deposition of the catalyst.[52,61–62]

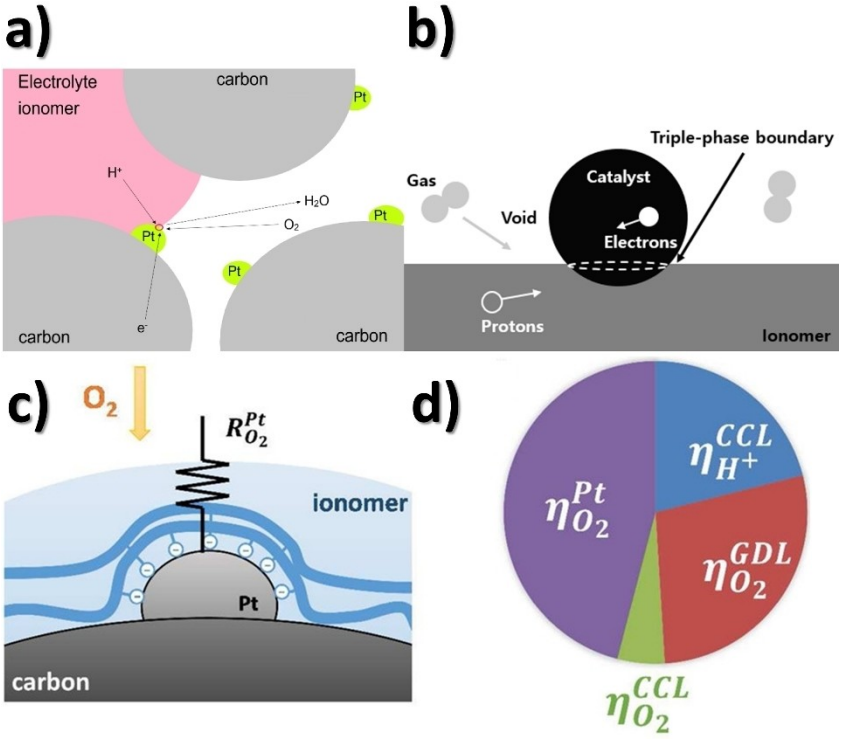

Figure 2. a) & b) Poor interpretation of TPB or rather ORR reaction site in the literature. Adapted from [57] and [19], respectively, distributed under a Creative Commons Attribution License (CC BY); c) Close-up view of the local O_2 transport to a Pt nanoparticle through the ionomer film; d) Simulated mass-transport voltage losses. Adapted with permission from reference [58]. Copyright 2016 American Chemical Society.

The preparation of the MEA also has a significant impact, as the aim is to achieve a close contact between the CLs and the PEM that enables efficient H^+ transport and electron conduction. This is possible as the gaps, voids or air pockets between the CLs are minimised, allowing for better physical and electrical coupling. This reduces the contact resistance at the interface and enables efficient electron transfer between the CLs and the conductive support material within the layers.[52,63] However, it needs to be noted that at high current density PEMFC operation reduction of those void may not necessarily enhance the performance due to hindered water management. Effective water management is crucial to prevent catalyst deactivation. It reduces the availability of catalyst sites by hindering the diffusion of reactants.[9]

The conditioning of PEMFC is primarily about minimising all existing resistances or maximising the TPB and achieving a stable state of the PEMFC components. The activation of the catalyst surface, the hydration of the membrane and ionomer and flushing out of impurities from the catalyst surface are considered to be among the critical processes.[52] This process can take only a few seconds or even hours, depending on the severity of the impurities already present, the location (CL or membrane), the catalyst (Pt or Pt alloy) etc.[36,64] Contaminating cations such as Fe^{3+}, CO^{2+}, Ni^{2+}, Cu^{2+} and Cr^{3+} can enter the ionomer and membrane via various sources. Unstable catalyst alloys such as PtNi or PtCo, water impurities and intentionally added cation sources such as cerium (Ce), which is used as a radical scavenger in PEM, can introduce these contaminating cations.[5,65–66] It has been observed that these cations preferentially replace H^+ in the ionomer, resulting in of H^+ conduction impediment through the sulfonate groups of the ionomer and hindering O_2 transport within the CL. Cation contamination can also influence the electroosmotic drag, which can support the hydration of the membrane. These processes often pose a major challenge and are the major bottlenecks in conditioning for optimal performance of the PEMFC stack.[5,67]

To date, the most commonly used polymer group for membrane and ionomer materials are the so-called perfluorinated sulfonated polymers or also perfluorosulfonic acid polymer (PFSAs). In the hydrated state, PFSAs have a relatively high H^+ conductivity and adequate gas permeability, which enables efficient diffusion of O_2 towards the catalyst sites. The best known polymer from this group is the commercially available Nafion.[68] In recent years, however, a many new modified versions of the PFSAs has emerged, e.g. the commercially available Aquivion[69] or Fumion,[70] or even new generation of polymers for PEM applications, e.g. hydrocarbons as Pemion.[71] However, it is important to note that thin ionomer layers show significant differences compared to the bulk material, especially in terms of water uptake and H^+ conductivity when the thickness is below 100 nm.[72] Consequently, new break-in protocols will be needed, potentially less demanding.

The most important prerequisite for ORR is the establishment of the TPB. However, to make the reaction feasible, all existing resistances such as the ohmic resistance (R_Ω), the H^+ resistance or the mass transfer resistance, which can occur e. g. due to the low porosity of the CL or the low hydration of the ionomer and the membrane, must also be reduced.[58] Accordingly, it is necessary to investigate a variety of mechanisms that influence the TPB and the critical resistance.

2.2. Possible Processes/Mechanisms Occurring during the Break-In

It is important to note that in order to optimise the break-in process of a PEMFC stack, it is essential to have a comprehensive understanding of both the beneficial/desirable and degradative mechanisms. Whilst the beneficial mechanisms improve the performance of the cells, it is equally important to identify and address the degradative mechanisms that can limit efficiency and lifetime. This multidisciplinary approach combines knowledge from electrochemistry, materials science and engineering fundamentals. It enables the development of strategies that strengthen the favourable mechanisms and at the same time weaken the degrading mechanisms and thus improve the performance and service life of the cells. At present, there is still much room for improvement in the field of PEMFCs, so that many changes in the design can be expected, such as thinner layers, optimised flow fields, etc. In this way, there is no "one fits all" solution for the break-in. It is therefore important to understand the possible mechanisms that help to optimise the individual case. By integrating this knowledge into the process, it can be ensured that the PEMFC realise their full potential and deliver efficient and reliable power generation over a long period of time.

In PEMFCs, the membrane and the anodic and cathodic CLs are the key components in the break-in process. Since the activation/degradation processes are closely intertwined, to decipher them we need to consider each key component separately: the membrane and the CL. On the other hand, we can further subdivide the CLs into the catalyst and the ionomer, and the catalyst into Pt/Pt alloy nanoparticles and carbon support material. For the membrane, the main activating processes are hydration and removal of impurities/contaminants, which are accompanied by subsequential processes such as membrane swelling and structural changes. In CL, on the other hand, the main process is the reduction of surface oxide on the Pt, hydration of the ionomer and removal of impurities, together with swelling of the ionomer – pore swelling, reorganisation of the catalyst and ionomer, increase in CL porosity, reduction of contact resistance at the interface, etc.

2.2.1. Membrane

The most important activation mechanism that influences the membrane is hydration. It has a major influence on the H^+ conductivity, as the H^+ conductivity in a dry PEM is almost zero. Accordingly, the operation of a PEMFC is strongly influenced by RH, which affects the H^+ conductivity of both the PEM and the ionomer.[73] The thickness of the membrane also has a major influence on water uptake and H^+ conductivity.[36] The sulfonic acid groups ($-SO_3H$) at the end of the side chains of the ionomer polymers in presence of water undergo the dissociation into H^+ and sulfonate ions (SO_3^-). The mobility of these H^+ ions within the material enables ion conduction through the polymer matrix, which is a crucial prerequisite for the reaction.[18,34] The polymer backbone, polytetrafluoroethylene, also known as PTFE, gives the ionomer hydrophobic properties, which means that the location of the absorbed water depends on its orientation.[74–75] On the one hand, the orientation of the side chains towards the catalyst promotes the contact of H^+ with the ionomer, on the other hand, this orientation can also lead to a certain degree of poisoning of the catalyst with SO_3^- (Figure 5).[75] The hydration of the rate also influences the state of the surrounding water. In contrast to water vapour, water in the liquid state affects the surface skin of the polymer and increases its hydrophilicity, so that the H^+ conductivity increases.[76]

Hydration also leads to swelling of the membrane, which increases the hydrophilicity of the membrane by forming a network of water-filled channels, which improves H^+ conductivity.[74] However, swelling can lead to dimensional changes that can potentially compromise the mechanical integrity of the membrane. On the other hand, insufficient hydration can lead to membrane shrinkage and increased stiffness, which can result in cracking or loss of flexibility.[77] Improper water extraction can also lead to water accumulation in the MEA, resulting in flooding and loss of porosity in the GDL or the ability of reactants to reach the CL.[78] In addition to the exchange of H^+ ions across the membrane, water molecules also permeate through the membrane, which is facilitated by electroosmosis. Excess water on the cathode side can lead to water transfer from the cathode to the anode. This leads to insufficient reactants reaching the active reaction area of the catalyst, resulting in reduced performance.[18] In certain cases, this mechanism can even be used as a membrane activation mechanism.

Among other factors that influence the hydration of the membrane, an increase in T generally promotes hydration as it increases the mobility of water molecules and facilitates their diffusion into the membrane. However, too high a T can lead to water loss through evaporation or structural changes of the polymer due to glass transition. The duration of the break-in also affects the degree of hydration; longer break-in phases allow for more extensive water absorption and swelling of the membrane, which leads to improved performance.[36,79] With different conditioning or even operating factors, water management is of great importance as it is necessary to maintain the optimum water content to avoid drying out or flooding of the PEMFC.[80] Therefore, prolonged hydration not only leads to over-swelling but also to flooding of the PEMFC, which additionally hinders the gas pathway and slows down diffusion.[81]

Conditioning PEMFC with Pt alloy-based catalysts can lead to degradation, although the loss of the intrinsic activity and electrochemically active surface area (ECSA) is by no means the only consequence. Dealloyed metal ions can poison the membrane by blocking the H^+ channels in the membrane by bonding to the SO_3^- side chains, resulting in a loss of proton exchange capacity. Metal ions can also contribute to the formation of hydroxyl radicals (OH•) in the membrane, leading to significant degradation of the membrane by catalysing Fenton-like reactions or decomposing hydrogen peroxide (H_2O_2) to OH•. The presence of radicals in the polymer membrane can initiate unzipping mechanisms.[65] There are several mechanisms that explain how OH• species can cause the degradation of a defect-free PFSA polymer: Formation of sulfuric acid (H_2SO_4) which lowers the pH and generates radicals that decompose into OCF_2 (perfluorooctanoic acid) fragments. Another possible outcome is the formation of H-radicals, which then react with the PFSA side chains. As a result, hydrofluoric acid (HF) is formed in addition to OCF_2 and SCF_2. Finally, sulphurous acid (H_2SO_3) could be formed, which triggers the subsequent degradation.[82] The effects are less pronounced in Pt alloy nanoparticles with core shells, as the Pt shell layer protects the Pt alloy core from leaching less noble metal.[83]

Higher operating T can promote the formation of OH•. In addition, changes in RH, gas flow rates and cell potential can influence the kinetics of the electrochemical reactions and thus the formation of OH•.[84] Therefore to improve the chemical stability of the membrane, radical scavengers can be used. These radical scavengers, such as transition metal oxides, are able to neutralise free radicals such as OH• and O_2H•, and thus prevent their damaging effects on the ionomer chains. Cerium and manganese oxides are commonly used as chemical stabilisers in this context, increasing the membrane's tolerance to radical attack and thus improving its overall chemical stability.[85] The use of these countermeasures opens the way for a tougher approach to conditioning, leading to a faster approach.

2.2.2. Catalyst Layer

For optimal cell performance, it is essential to have well-intertwined pathways of all three key components: protons

through the ionomer, electrons through the catalyst and supporting materials, and oxygen through the gaseous phase. These pathways should intersect frequently or have minimal resistance, such as the diffusion of oxygen through the ionomer layer to the catalytic sites.[51]

Although the membrane and the ionomer are usually made from a similar material, sometimes even from the same material, there are major differences in functionality. The ionomer must still achieve a high H^+ conductivity, but unlike the membrane, it must also be able to allow gas, more specifically O_2, to pass through. To a certain extent, this is achieved by using it as an electrolyte "thin film".[86] The main goal of the ionomer is therefore high H^+ conductivity and ensuring complete coverage of the catalyst particles. Similar to the membrane, hydration (Figure 3) is essential for maintaining the H^+ conducting properties of the ionomer. Adequate water content ensures that the ionomer remains in an ionically conductive state.[87] While the presence of $-SO_3H$ groups in close proximity to the catalyst surface facilitates the transport of H^+, the SO_3^- groups can bind to the Pt surface and subsequently poison it.[43] This can reduce Pt activity by 2 to 4 times compared to its original level.[36]

In addition to increasing ionic conductivity, hydration also stimulates swelling of the ionomer (Figure 3), where the pores enlarge and consequently gas transport is enhanced.[88] If swelling continues until an excessive threshold is reached, there is a possibility that the pore size within the CL structure will be reduced and gas diffusion to the catalyst sites will be hindered, which leads to mass transport limitations. In extreme cases, swelling could also lead to deformation, cracks or delamination. If the PEMFC continues to run, the ionomer reaches a stable state in which its swelling is compensated by the water content and the operating conditions.[18,74]

When the membrane and the ionomer swell, the catalyst particles present in the electrode unit can redistribute. The expansion of the ionomer can push the catalyst particles so that they are distributed more evenly in the CL. In the case of the Pt/C catalyst, this redistribution contributes to a more even distribution of the catalyst particles, which in turn improves the availability of catalytic sites for the gaseous reactants. During the break-in process, the redistribution of the catalyst - the movement or rearrangement of the catalyst particles - can also be triggered by many other factors such as T, p and degree of hydration. While catalyst redistribution is

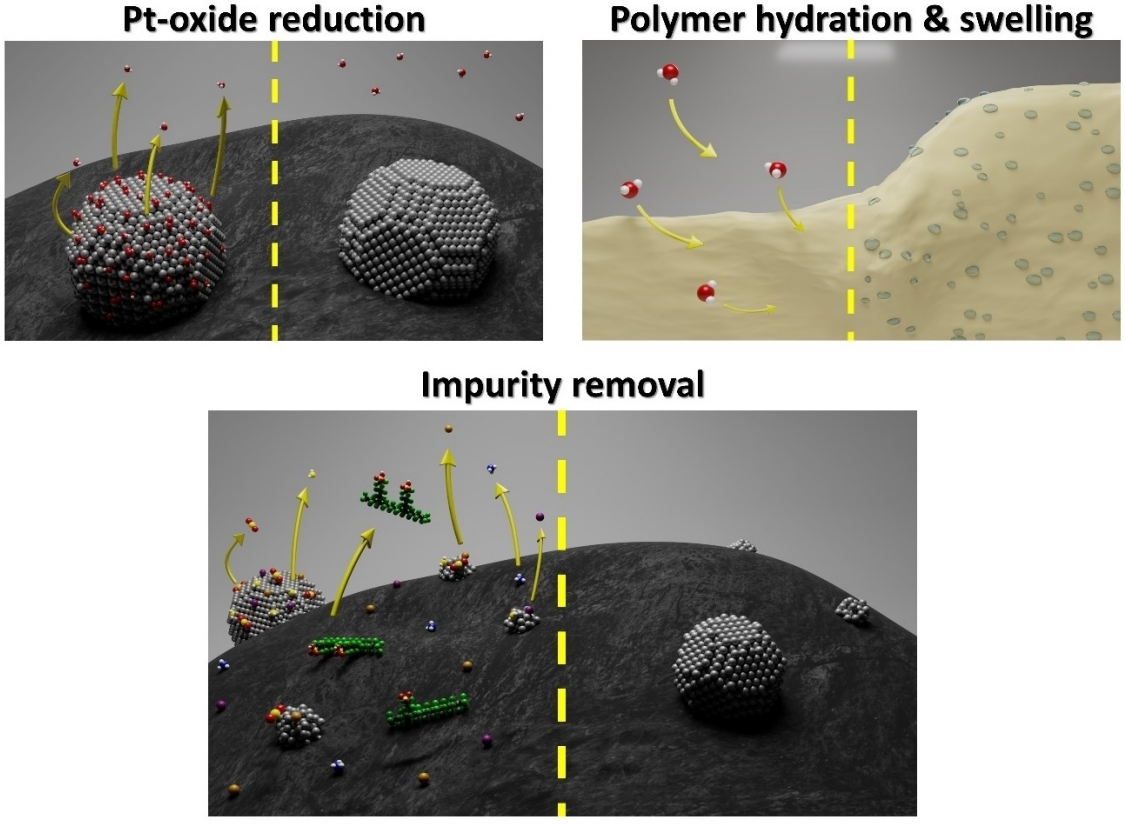

Figure 3. The main activating mechanisms for break-in of PEMFC: Pt-oxide reduction – reduction of O, O_2 and OH species from the Pt surface; polymer hydration and consequential swelling; impurity removal – leaching of contaminants such as metal ions (Fe^{2+}, Co^{2+} etc), polymer residues, SO_2, H_2S, NH_3, etc.

generally beneficial in the case of Pt/C, excessive movement of the catalyst particles can lead to their agglomeration or clumping.[89]

Carbon oxidation :

$$C^{*} + H_2O \rightarrow C\ OH + H^{+} + e^{-} \mathrm{E} = 0.2\ \mathrm{V_{RHE}} \quad (4)$$

Pt oxidation :

$$Pt + H_2O \rightarrow Pt\ OH + H^{+} + e^{-} \mathrm{E} = 0.7\ \mathrm{V_{RHE}} \quad (5)$$

The next important activation process besides the hydration of the polymer is the reduction of the oxidised Pt surfaces (Figure 3), which plays a major role in improving the ORR on the Pt surface; break-in of the PEMFC.[90] The duration of the reduction process can vary depending on the adsorbed species and locations and can resolve in seconds or even up to 20 minutes.[91,92] Figure 4 shows a typical Pt cyclic voltammogram in which all the important reactions triggered by a specific voltage are marked.[93] The reduction of the oxidised Pt is directly influenced by the applied voltage. At a potential below 0.65 V, the dominant species on the Pt surface is $H_2O_{(ad)}$; above 0.65 V, $OH_{(ad)}$ is formed by the oxidation of $H_2O_{(ad)}$; and at potentials above 0.8 V, $OH_{(ad)}$ further oxidizes to $O_{(ad)}$.[88,94] These species block the surface and lower the ECSA, so their removal is crucial. Therefore, lowering the voltage to low voltages, below 0.6 V, reduces the oxides on the Pt surface.[95] The voltage sweep at lower voltages may not prove beneficial in conditioning FC, but has proven useful in diagnostics for calculating ECSA using hydrogen underpotential deposition (HUPD) or rather using hydrogen adsorption/desorption peaks (Figure 4).

Impurities that have a negative effect on PEMFCs can take the form of carbon monoxide, carbon dioxide, ammonia, sulphates, phosphates, metal cations, PFSA polymer residues, etc. These impurities have a detrimental effect on ORR kinetics and lead to reduced Pt activity. Many of these impurities can be introduced into the PEMFC during production, including metal cations and PFSA residues or can be introduced to the system in another way like from hydrogen fuel or air oxidant. Another important factor of break-in is therefore the rinsing out of impurities present in the CLs (Figure 4).[96–97] Unlike the membrane, the CLs contain the main source of impurities, the catalyst. Possible impurities are various residues from all previous production stages, e.g. acids or less noble metals from catalyst production,[12,98] or solvents from ionomer production.[99] The catalyst also generates hazardous residues during break-in phase by releasing less noble metals. These are known to promote polymer degradation by catalysing the formation of OH radicals,[5] adequate rinsing is an essential part of break-in.

It is important to note that reducing the Pt loading, which is necessary to reduce costs, can make the system more susceptible to degradation, resulting in higher degradation rates being observed.[100–101] However, regarding the influence of the I/C ratio (ionomer/catalyst), theory shows that the current density and Pt loading have a linear dependence, provided that the ionomer content is within an optimal range. If the ionomer content is too low, it can hinder the H^{+}

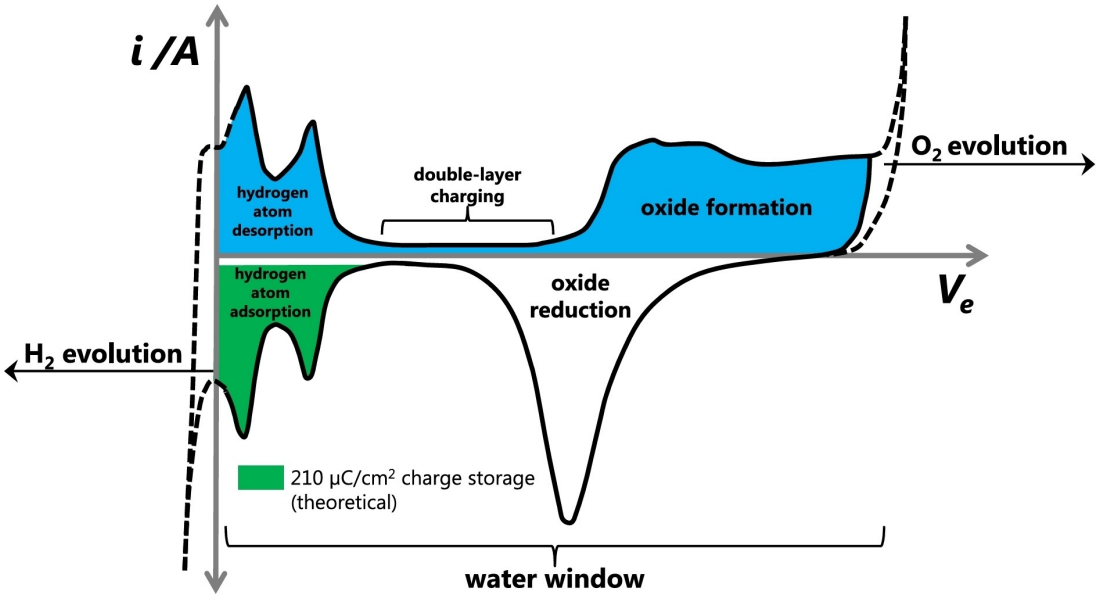

Figure 4. Typical cyclovoltammogram of Pt electrode. Reprinted from reference [93] under the terms of the Creative Commons Attribution 3.0 International (CC BY 3.0) license. Copyright ©2016 IOP Publishing Ltd.

conductivity and have a negative effect on the current density.[58,102] It has also been shown that Pt without ionomer coating is more susceptible to degradation in the absence of liquid water.[46] However, if the ionomer content is too high, it can hinder O_2 diffusion and thus also affect the current density. With high Pt loading and high ionomer content, the limiting factor for performance shifts from H^+ conductivity to diffusion losses through the plane - Knudssen diffusion of O_2.[58,102]

Compared to the membrane, the CL exhibits much more complexity and potential degradation processes.[103–104] Degradation can be accelerated by conditioning factors, such as elevated T, voltage cycling - especially high voltage - and high RH.[100] Increased T can promote electrochemical dissolution, the rate of which increases exponentially between 65 °C and 80 °C.[105–106] It can also lead to agglomeration of the catalyst.[107] The primary degradation mechanisms of CL (Figure 5) are Pt dissolution, Ostwald ripening, migration of particles followed by coalescence and potential sintering, and particle detachment associated with de-alloying, carbon corrosion, ionomer degradation and the migration and precipitation of Pt into the polymer membrane.[44,104,108] Electrochemically induced Ostwald ripening involves the dissolution of smaller Pt nanoparticles and the deposition of dissolved Pt species on larger nanoparticles. This process leads to a general growth of the larger particles at the expense of the smaller ones. The dissolution of Pt is one of the most complex degradation mechanisms that occur during the operation of PEMFC.[109] Although Pt is a noble metal that is relatively resistant to oxidation, unlike other materials, thermodynamic considerations based on the Pourbaix diagram nevertheless indicate that Pt can indeed be oxidised and even dissolved under the potentials and pH conditions relevant to PEMFCs.[110] However, the majority of dissolved Pt is not due to its thermodynamic properties, but to so-called transient processes triggered by the formation and subsequent reduction of O_2 species below the surface during voltage cycling.[111]

The induction of higher voltages, close to the open circuit voltage, also called OCV (theoretical value: ~1.23 V; practical value: ~0.95–1.05 V),[112] can lead to Pt dissolution.[113] It is caused by Pt oxidation and carbon corrosion, which subsequently leads to the growth of nanoparticles due to Ostwald ripening.[35,109] Therefore, cycles with lower current density or higher operating voltage accelerate the growth of Pt particles. Maintaining the voltage at OCV leads to drying of the membrane due to the low current conditions, resulting in low water formation.[114] In addition, significant deposition of dissolved Pt from the cathode into the membrane occurs during cycles with longer OCV hold times, which could be due to re-deposition of Pt during drying of the PEMFC[110,115] On the other hand, the application of lower voltages increases the H_2 consumption and thus also the break-in.[88]

The next mechanism is the detachment or loss of Pt particles from the carbon support due to various factors such as corrosion of the carbon carrier or mechanical stress. The detached Pt particles can then be redeposited on the electrode or lost.[115] Carbon corrosion at the site carrying the Pt particles where the reaction enthalpy can be reduced in the presence of catalysts. During voltage cycling, a partial oxide layer gradually forms between the carbon support and the Pt nanoparticles, leading to a reduction in adhesion.[116] The next mechanism is migration of crystallites, followed by coalescence, where Pt crystallites can migrate on the carbon support due to the electrochemical potential gradients. Moving crystallites can coalesce with other Pt particles in the vicinity, leading to their growth.[115]

The dissolution and redeposition of Pt is effectively suppressed during loading cycles at lower RH, primarily due to the lower water content in both the ionomer and the membrane. This reduction in water content hinders the transport of Pt ions and suppresses Pt oxidation. Subsequently, it has been suggested that Pt degradation during load cycling can be mitigated by operating the PEMFC at a reasonably low RH, even when the OCV is held for extended periods of time.[110] Nevertheless, excessive movement of the catalyst particles during redistribution can potentially cause damage to the membrane-electrode interface. Mechanical stress or abrasion from particle movement can compromise the integrity of the membrane, resulting in reduced H^+ conductivity, increased leakage and reduced cell durability, especially for thin membranes in the 10 µm range.[117,118]

Knowledge of PEMFC and break-in phase is primarily based on Pt-based catalysts, with a lack of research into Pt alloy applications. Accordingly, there is still a significant knowledge gap regarding the applicability of these findings to more complicated PtM/C nanostructures (where M stands for an early or late transition metal, e.g. Cu, Ni, Co, etc.). For catalysts based on Pt alloys instead of pure Pt, there are certain advantages, such as strain effect and the dilution of the Pt in the core of the nanoparticles,[119] but at the same time many new complexities arise, such as the dissolution of less noble metal along with all of its consequences.[120] Pt alloys, if not properly dealloyed/activated[12] during catalyst production, can also extend break-in time and require a higher number of cycles for optimal performance. However, voltage cycling can also lead to a degradation.

In a study by Gummalla et al.,[121] the distribution of deposited Pt was found to be different between the two catalyst types. In particular, the use of PtCo/C catalyst led to a decrease in MEA conductivity, which was not observed with Pt/C catalysts. When PtCo catalyst was used, Pt particles with a size of 10 to 35 nm were evenly distributed in the membrane. In contrast, when pure Pt catalyst was used, a 2.5 micrometre wide Pt band was observed near the cathode.[109]

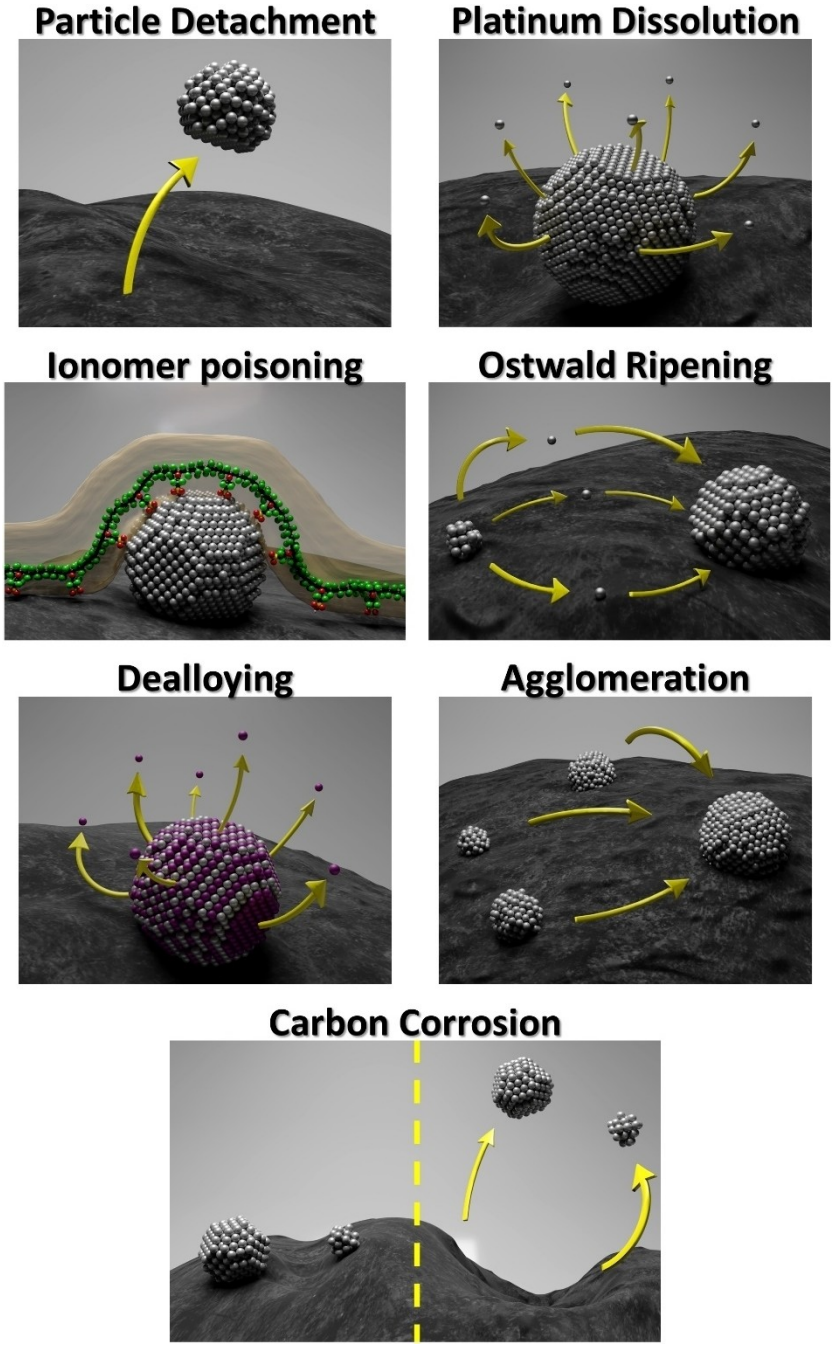

Figure 5. Degrading mechanisms present in PEMFC during the break-in: particle detachment, platinum dissolution, ionomer poisoning (SO_3^- from ionomer side chains bonding Pt surface), Ostwald ripening, dealloying, agglomeration, carbon corrosion.

In-situ synchrotron X-ray fluorescence analysis, also known as XRF, showed that Co^{2+} ions are not only mobile in the in-plane direction but also in the through-plane direction of the membrane.[122] The dissolution of Co^{2+} leads to contamination of the ionomer phase with it, where they increase the mass transport resistance of H^+ and O_2 in the electrode. In particular, the ion exchange process involving SO_3^- and Co^{2+} in the catalyst layer ionomer leads to reduced water uptake and consequently to a decrease in the volume of the hydrophilic domain.[5,123] Moreover, this process also induces O_2 transport resistance by obstructing O_2 pathways (Figure 6). In case of multivalent metal cations such as M^{2+} or M^{3+}, cross-linking

between adjacent PFSA side chains or rather SO_3^- occurs (Figure 6). Multivalent metal cations also present higher poisoning rate of ionomer as each cation bonds with several SO_3^-.[5] Mitigating cobalt dissolution and contamination is crucial for improving the performance and lifetime of PEMFC, especially for heavy-duty automotive applications.[124]

The presence of internal porosity in porous carbons allows the deposition of a significant number of catalyst nanoparticles inside the pores. When the ionomer is incorporated into the electrodes, it does not effectively penetrate these small pores to come into contact with the Pt nanoparticles inside.[55] Since the catalyst in the pores is not covered with ionomer, it is not poisoned by it, which increases its activity. The lack of contact with the ionomer also does not mean that there is a lack of H^+, as these are still delivered by water accumulated in the pores. The pores can have very small openings, ranging from 1 to 4 nm, and the structure of the pores themselves can be intricate and tortuous. Accordingly, it strongly depends on the size and accessibility of the pores. In smaller pores, gas transport is limited due to inaccessibility (Figure 7) and in large pores, H^+ conductivity is limited as the ionomer has a hard time reaching the sites inside. Mesoporous carbons have a pore size that falls right in between, resulting in improved activity without hindering the transport of H^+ or O_2.[55,125] Mesoporous carbon provides a great anchoring surface for catalyst nanoparticles by trapping them within the pores, improving resistance to metal dissolution.[55,126] However, the corrosion rate of carbon materials tends to increase with higher

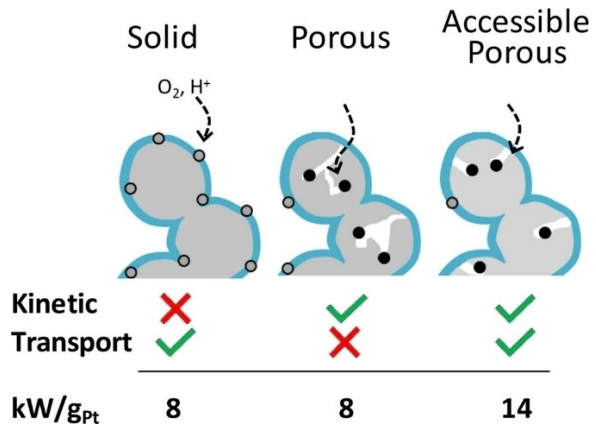

Figure 7. ORR kinetic and transport (O_2 and proton) characteristics of catalyst layer structures made from three types of carbon (gray). Small black and gray circles represent relatively high and low activity Pt particles, respectively, due to ionomer (blue) adsorption. Reprinted with permission from reference [55]. Copyright ©2018 American Chemical Society.

specific surface area (m^2/g) due to the higher number of susceptible oxidation centres, making mesoporous carbon more susceptible to degradation.[127–128] This oxidation can be triggered by high voltage (above 0.65 V),[129] or free OH radicals forming carbon dioxide (CO_2) or other oxidised species.[130–131] In addition to oxidation, free radicals can also react with water and cause the formation of H^+, resulting in increased acidity, which also causes carbon degradation.[132] In

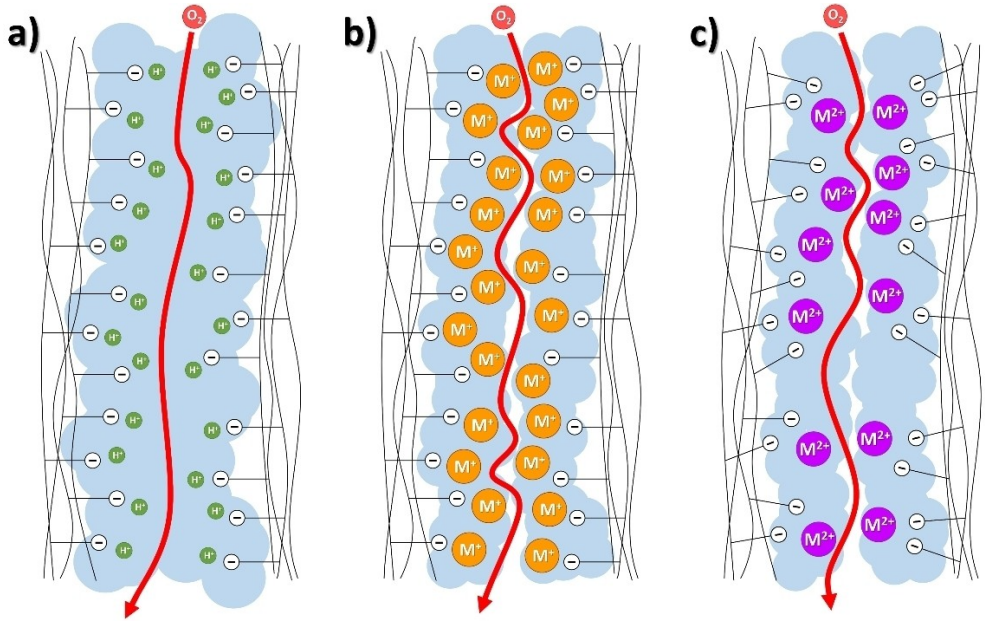

Figure 6. a) Fully humidified ionomer; b) fully humidified monovalent contaminant cation-form ionomer; c) fully humidified multivalent contaminant cation-form ionomer. Scheme inspired by [5].

this way, the choice of which mechanism is favourable for the establishment of TPB in a given system, or how the break-in procedure should be carried out, also depends on the porosity of the catalyst support material.[55]

It should be noted that the research work is usually based on a smaller scale, such as half-cells (TF-RDE, gas diffusion electrode - GDE) or smaller MEA test stations, which are idealised examples of PEMFC. In real systems, however, there is much more inhomogeneity and complexity. Furthermore, one cannot simply rely on the measured power output to achieve an optimal break-in. Instead, one must understand the activation/degradation mechanism of certain break-in. Knowledge about the state of the PEMFC at the micro/nano level can be obtained by various *ex-situ* methods, which are explained in the following chapter.[133]

3. Analytical Approaches

In this chapter, we will focus on analytical techniques that help to decipher the processes that influence the performance of the PEMFC stack during the break-in phase. By using the following methods in synergy with computational modelling, an understanding of the electrochemical phenomena unfolds. As break-in turns out to be a series of different complex processes.[5,134–135] we accordingly need a variety of *in-situ* and/or operando techniques. On the one hand, we can gain valuable insights with half-cell setups such as TF-RDE,[136] GDE,[134,137–138] modified floating electrode (MFE)[139–140] or full-cell methods at the PEMFC test station such as electrochemical impedance spectroscopy (EIS).[141–142] On the other hand, we can also break down the PEMFC into individual components and analyse them piece by piece *ex-situ* using other analytical techniques such as Raman spectroscopy,[129] X-ray diffraction analysis (XRD),[143] small-angle X-ray scattering (SAXS),[108,144] wide-angle X-ray scattering (WAXS),[145] X-ray photoelectron spectroscopy (XPS),[44,146] inductively coupled plasma mass spectrometry (ICP-MS),[137] scanning electron microscope (SEM),[147] energy-dispersive X-ray spectroscopy (EDS),[148–149] focussed ion beam scanning electron microscope (FIB-SEM),[150] electron-probe microanalysis (EPMA),[124] transmission electron microscopy (TEM),[151] scanning transmission electron microscopy-electron energy loss spectroscopy (STEM-EELS),[152] cryo-electron tomography (cryo-ET)[153–154] etc.[36,124,155–157]

In an attempt to simulate the processes taking place in a real PEMFC, some analytical techniques based on the half-cell principle have been developed (Figure 8). For instance, the TF-RDE can serve as a simplified and idealised representation of a half PEMFC for testing the electrocatalyst.[48] This configuration provides a valuable means of rapidly evaluating the activity and stability of novel catalysts, using only small amounts of material (µg scale per measurement) in the initial development stages. Using a liquid electrolyte for this characterisation bypasses the complicated MEA manufacturing process, which requires specialised laboratory equipment and expertise.[158] Such early stage screening on the TF-RDE allows the performance of the catalyst to be evaluated before larger scale production is initiated and more extensive *in-situ* evaluations are carried out in a complete PEMFC plant. The method also allows the simulation of harsh conditions that occur during the operation of PEMFCs or the simulation of processes that occur on a catalyst during break-in.[155,159] However, in contrast to the TF-RDE configuration, this performance is not only influenced by the state of the catalyst surface, but also by various other parameters of the MEA, such as the hydration of the membrane and ionomer, which affect the H^+ conductivity, as well as by impurities introduced during assembly and by dealloying particles.[155]

In practical scenarios, ORR activity is measured at significantly higher overvoltages, typically between 0.6 and 0.7 VRHE. The currents in an operational PEMFC are at least two to three orders of magnitude greater than those observed in TF-RDE measurements. In TF-RDE evaluations, the mass transport of gas reactants such as O_2 and H_2, which have relatively low water solubility, is significantly hindered.[140] On the other hand, GDE is more comparable to real PEMFC as it offers higher currents, more realistic mass transport and TPB. On the other hand, it requires higher complexity in measurement, e. g. coating the catalyst on the GDL, which requires the use of a spray coater.[134] On the other hand, GDE serves as a bridge between fundamental studies with TF-RDE and applied research with MEA. It enables targeted investigations of CL stability and selectivity phenomena under conditions relevant to mass transfer.[134]

Similarly, there is another advanced analytical technique, namely MFE, which helps to improve the fundamental understanding of ORR activity and the stability of an electrocatalyst.[160] The method is a modification of the floating electrode (FE) method.[160,161] The analytical technique involves rapid mass transport to an extremely low catalyst loading layer as the electrode is buoyant in the liquid phase. Consequently, the gaseous reactants are fed almost directly from the gas phase or at least through an extremely thin liquid layer, resulting in remarkably high specific ORR current densities.[139,160] Furthermore, in contrast to FE, the MFE approach allows the use of subsequent non-electrochemical diagnostics. It could be coupled with advanced structural characterisation, such as transmission electron microscopy at identical locations (IL-TEM).[140]

If we continue to follow the development of PEMFC, we come across a very useful analysis technique called EIS. It is not only an effective tool for fundamental understanding of PEMFC, but also for performance diagnosis. It is characterised as a versatile tool with high sensitivity to a variety of factors.

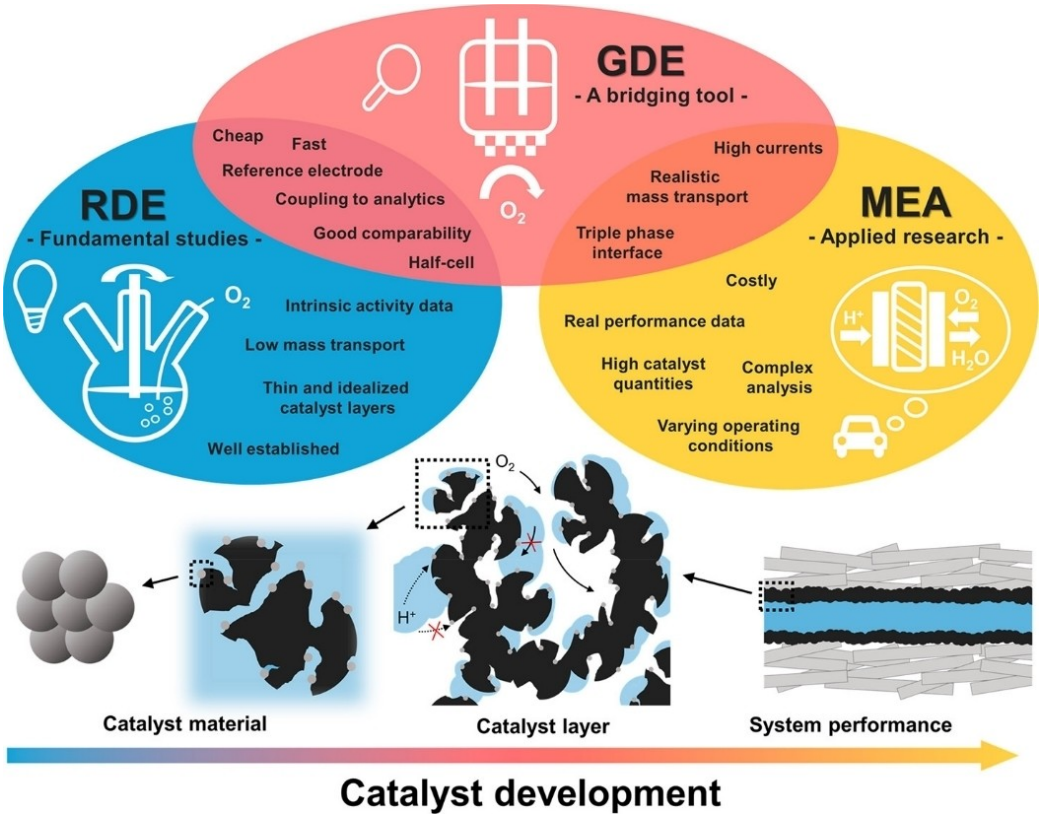

Figure 8. Comparison of different levels of electrochemical catalyst (layer) evaluation. Reprint with permission from reference [134]. Copyright 2022 American Chemical Society.

EIS can be operated *in-situ* and non-invasively and enables real-time monitoring of both external operating conditions and internal core components in PEMFCs.[141,162] Monitored external operating conditions include clamp compression, break-in protocol, operating T, gas RH, electrical load, gas p, gas stoichiometry, reactant contamination and water content. Key internal components observed include catalysts, CLs, GDLs and bipolar plates.[142] The resulting data reflect the sum of the various physicochemical processes within the PEMFCs, resulting in global sensitivity and significant overlap in limited frequency ranges. This complexity can be challenging to interpret.[163] Online method, namely micro-current excitation (MCE), has shown great promise in measuring parameters such as catalyst roughness factor (RF) – number of active sites, R_Ω – ionic resistance of ionomer and membrane, H_2 crossover current density (i_H), double-layer capacitance (C_{dl}) and short-circuit resistance (R_e) – resistance of membrane to electron transfer.[164–165]

The analytical technique, μ-Raman spectroscopy,[166] is known for its direct sensitivity and specific ability to detect water. Actual resolution of a few micrometres in each direction is reported in the literature, which is found to be essential for independent studies at the channel and rib (also called "land") sites.[167] The analytical technique is used, for example, to monitor the degradation of carbon carriers.[45,129] However, with the use of appropriate optics and refined data processing techniques, both in-plane and through-plane resolution could be significantly improved, with the diffraction limit of the optical setup being improved to ≤ 1 μm. In the context of state-of-the-art membranes with a thickness of 25 to 50 μm, this higher resolution is essential for thorough investigations at the membrane-water interface. The main challenge with the *in-situ* μ-Raman method is its intrusiveness, as it requires the removal of all light-absorbing media along the optical path.[167]

The Brunauer–Emmett–Teller (BET) technique is generally used to measure the specific surface area of materials by physically adsorbing gas molecules (usually nitrogen or argon) on the surface of the material. In the case of break-in, it can be used to determine changes in porosity catalyst in CL at the nanoscale.[55,168] On the other hand, mercury intrusion porosimetry (MIP) could be used to observe the porosity of whole CL.[169] In contrast to BET, it is known as a destructive method, which unfortunately means that it cannot be used to study the same exact material before and after the procedure.

However, these techniques only provide bulk property information.[170]

The XRD analysis technique proves to be a fast and decisive approach to evaluate the stability of a catalyst by determining the size of the metal particles. The catalytic activity is highly dependent on the shape, size and distribution of these metal particles, and it can provide information on particles smaller than 10 nm.[148] The disadvantage of XRD is the relatively large penetration depth, which is about 1 mm. With a high penetration depth, it is more difficult to distinguish parts of the MEA.[143] On the other hand, by using a much stronger X-ray beam or synchrotron X-ray radiography[171] it is possible to perform tomography of the entire MEA. This allows the position of even small water clusters within a PEMFC to be accurately determined, mimicking realistic operating conditions in terms of T and current density. In addition, the swelling of PEM and ionomer can be observed.[172] On the other hand, the latter analysis technique is extremely less available than others, as there are currently only about 70 synchrotrons worldwide.[173]

SAXS, in contrast to MEA or TF-RDE measurements, offers the possibility to analyse the CL without disassembling it, taking samples or even removing the membrane. The most important information provided by this analytical technique is the particle size distribution, which can indicate mechanisms such as coalescence and electrochemical Ostwald ripening.[108] SAXS is an analytical technique used to investigate structures and dimensions at the nanoscale. The combination with WAXS enables the acquisition of additional information about the atomic structure.[144] SAXS and WAXS can be coupled with a synchrotron that offers high X-ray transmission. This enables *in-situ* analyses without compromising cell performance. The 360° transparency within the sample plane enables imaging in conjunction with advanced techniques, including XRD computed tomography.[145]

Similarly, X-ray Absorption Spectroscopy (XAS), sub-techniques as Extended X-ray Absorption Fine Structure (EXAFS), are invaluable for investigating the electronic structure and chemical state of nanoparticles in PEM fuel cells.[174,175] These methods are particularly useful for studying the surface states and sizes of nanoparticles, which are crucial for catalytic efficiency and durability. EXAFS provides detailed information about the local atomic environment around specific elements, while NEXAFS is sensitive to the chemical states and bonding environments. These techniques are often cited in literature for their precision and ability to provide insights into the mechanisms of catalyst degradation and performance.

Additionally, neutron scattering and neutron imaging are a powerful technique for assessing the extent of catalyst layer flooding, which is critical for understanding water management and its impact on fuel cell performance.[78,176–178] It can provide unique insights due to its sensitivity to light elements like hydrogen, allowing detailed studies of water distribution and accumulation within the cell. This information is vital for optimizing the design and operation of PEM fuel cells to ensure efficient and reliable performance.

XPS is another analysis method that uses monochromatic X-rays. The energy of the X-rays is transferred to an electron in an inner energy layer, resulting in the ejection of electrons from the surface.[148] Surface-sensitive XPS measurements can provide detailed information about the composition and chemical state of the individual elements on the surface of the CL. Accordingly, it is used to observe morphological changes in the CL. This technique is very interesting as it gives an insight into the oxidation state of the Pt surface and thus can monitor one of the main mechanisms of break-in, the reduction of Pt oxides at the surface.[179] The migration of Pt can be observed by monitoring the increase/decrease of Pt content. The degradation of CL could also show up in the XPS spectrum as a loss of fluorine.[44] XPS is a surface technique, so the aforementioned findings are limited for research in the bulk of the material.[146]

The degree of activation or even degradation of the PEMFC stack during break-in could be determined by monitoring the composition of the outlet gas and water during the different stages of break-in using GC (or GC-MS) and ICP-MS, respectively. With the mentioned method we could for example estimate the gas transition rates. We could also monitor the decontamination of the ionomer and the catalyst surface by determining the concentration of various emissions (e.g. sulphate and other impurities). Similarly, emissions such as fluorine and H_2O_2 can be correlated with the degradation of the ionomer and the catalyst binder, while the CO_2 concentration can indicate the degradation of the carbon support.[137] An electrochemical cell coupled to a mass spectrometer (EC-MS) can also provide us with information on carbon corrosion by measuring the CO_2 signal. The technique allows the observation of all gaseous products generated during operation[180] and can therefore even be used to monitor the removal of contaminants such as organic solvent residues.

SEM enables the analysis of porosity and surface structure, allowing the pore structure, thickness and cross-sectional structure of the CL to be determined.[148] It can provide a qualitative insight into the microstructure of the CL with a resolution of 1–20 nm.[181] In principle, SEM is a non-destructive technique as long as the samples have good conductivity. SEM is often coupled with EDS, which provides information into the elemental composition of the electrode surface. EDS is a valuable technique that investigates variations in the elemental composition of a CL, whether due to particle migration, growth, accumulation of catalyst particles or degradation of PEMFC components.[148–149] To achieve higher

precision of the cross section, SEM is often coupled with FIB. This not only provides higher accuracy, but also enables the combination of image series for CL reconstruction. Once the SEM images are aligned and reconstructed, 3D visualisations can be created. FIB-SEM nanotomography could give us a better insight into the porosity, pore size distribution and tortuosity of CL, as we could only speculate with stand-alone SEM or rather use it for relative studies.[150,182] In the case of cross-sectional studies, the method called cross section polisher (CP) may be superior to FIB as it is able to obtain similarly accurate full cross-sections in a fast time frame.[183] There is even another modified method, namely Cryo-FIB-SEM, which is mainly used in the study of biological samples.[184] Unlike the standard method, it can provide information about the material in the hydrated state, making it the ultimate tool for studying the PEMFC structure after break-in in pristine condition.

EPMA is a powerful technique for the non-destructive chemical analysis of solid samples using focussed electron beams to generate characteristic X-rays. It is fundamentally similar to an SEM, but is a stand-alone device with the difference that it also offers the possibility of chemical analysis. Compared to EDS, which provides rapid qualitative analysis, EPMA provides precise quantitative analysis and phase identification.[185] It uses wavelength-dispersive spectrometry (WDS), which is more desirable for precise detection because EDS has limited spectral resolution (overlapping peaks) and sensitivity for many element combinations.[186] The key feature of an EPMA is its ability to perform precise and quantitative elemental analyses at remarkably small scales of only 1–2 microns,[187] although similar to EDS it can also be used at higher (micron) scales.[186] In the context of a PEMFC study, it could provide a detailed elemental distribution across the cross-section of the MEA. It can be used for a more detailed study of metal migration or dissolution/leaching.[124]

The use of TEM analysis is of great advantage when analysing the structure of PEMFC. It shows the spatial distribution of the individual components and allows the composition to be analysed at the nano or atomic level.[188–189] Accordingly, it allows the study of the most complex processes that are not detectable by other techniques, such as Ostwald ripening or carbon corrosion.[44] However, since the analysis takes place in vacuum, it is impossible to observe the hydrated ionomer, which complicates the study of TPB and the relationships between Pt and ionomer. Compared to previous methods, such as SAXS or WAXS, it does not provide an average size distribution of the whole CL without decomposition, but rather a localised insight. Thus, while we lose a more generalised/broad insight, we can observe the same particles *in-situ*.[108] However, it should be noted that the challenges related to sample preparation and potential damage to the samples by high-energy electrons should not be underestimated when using TEM.[148] A modified method, called IL-TEM, can enable an *ex-situ* study of the exact same nanoparticle before and after the process.[190]

By acquiring EELS spectra from different regions of the CL, the presence of certain elements (such as C, O_2 or S) and chemical states can be investigated. This information helps to understand the interaction between the ionomer and the catalyst particles and the influence of the ionomer composition on the performance of the PEMFC.[191] EELS can be used to analyse the changes in the composition and electronic structure of the CLs, the PEM and other components. It can provide information on the distribution and oxidation state of the catalyst particles, changes in the surface chemistry of the catalyst and the formation of reaction products. These insights help researchers to understand the evolution of the materials and their role in the break-in process.[152]

Cryo-ET is a technique that makes it possible to analyse the 3D structure of materials at cryogenic T, usually biological samples - cells, tissues or organisms.[153] Cryo-ET can be used to capture high-resolution, three-dimensional images of these components in their hydrated state, providing insights into their nanostructure, porosity and connectivity. In addition, Cryo-ET can also be used to study water management and distribution within the PEMFC stack. Water plays an important role in the operation of a PEMFC, and its distribution affects performance and durability. While the Cryo-FIB-SEM allows the investigation of PEMFC in pristine hydrated state on a larger scale, the Cryo-ET allows the investigation on a nanoscale, e.g. visualising the water distribution, including the formation of water channels or droplets, which can affect the electrochemical processes and the overall performance of the stack. In the context of studying the ionomer in PEMFC CLs, Cryo-ET can provide detailed information about its nanostructure and morphology. The PEMFC CL can be cryo-sectioned into thin slices and a series of tilted images are taken with an electron microscope. These tilted images are then computationally reconstructed to create a 3D model of the ionomer structure within the CL (Figure 9). Cryo-ET provides valuable insights into the distribution, orientation and connectivity of the ionomer at the nanoscale, revealing its relationship to the catalyst particles, pore structure and overall electrode architecture. This information helps to understand how the ionomer influences R transport, reactant diffusion and water management in the PEMFC.[154]

Cryo-ET is a technique that combines cryogenic sample preparation with TEM imaging to study samples under near-native conditions. In the case of a PEMFC stack break-in, cryo-ET can be used to visualise the structural changes and the distribution of the different components within the stack. Both STEM-EELS and Cryo-TEM techniques provide complementary information about the ionomer in PEMFC CLs. STEM-EELS provides chemical information and spatial

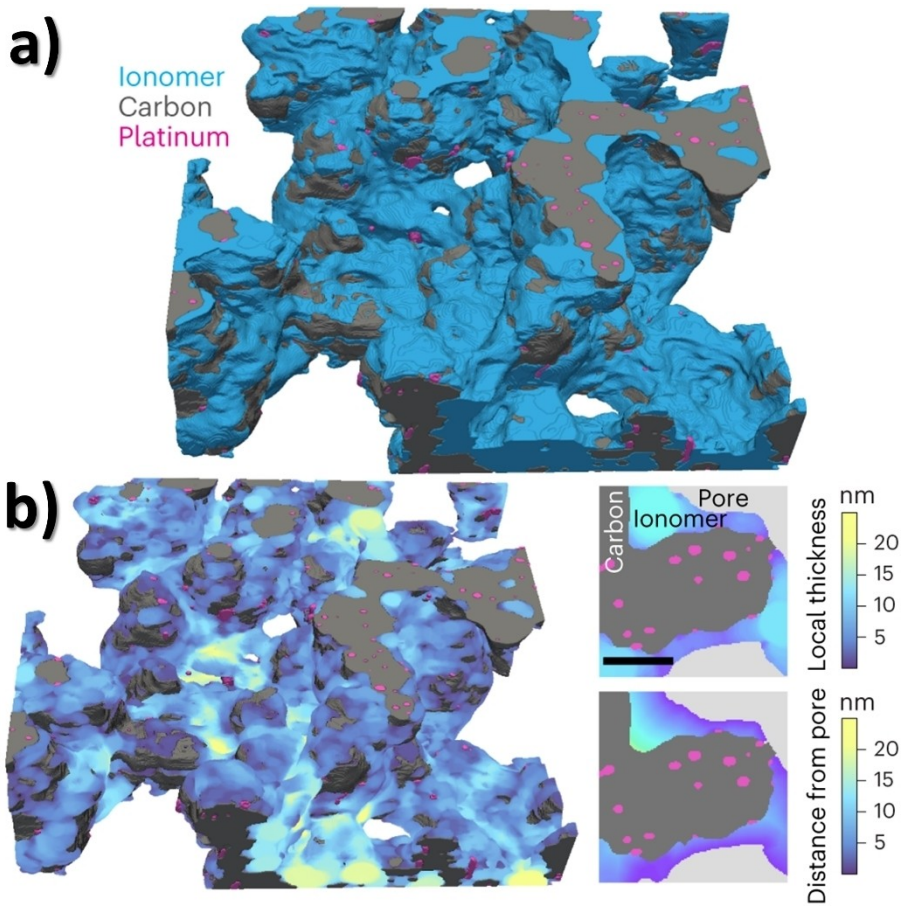

Figure 9. a) Segmented reconstruction of CL with Cryo-ET; b) A 3D map of the ionomer local thickness, and magnified images illustrating the difference in calculation to the local thickness algorithm, and a graph-based distance calculation from the external pore. Scale bar, 20 nm. Adapted from [154] under a Creative Commons Attribution License (CC BY).

analyses at high resolution, while cryo-ET provides 3D structural information in a near-native state. Cryo-ET is also known as non-destructive, as cryogenic T reduces the rate of radiolysis. Together, these techniques provide a comprehensive understanding of the role and behaviour of the ionomer in PEMFC, i.e. they are a truly powerful tool to study the changes that have taken place during run-in at the microscopic level, or the mechanisms that have taken place.[152,154]

Using the analytical techniques mentioned above, the development of complex models could be achieved. Computer modelling could further confirm the hypotheses about the mechanisms that take place during break-in, how they affect the PEMFC and how different parameters influence them.[192–194] These models could also help us to interpolate or even extrapolate[195–197] the knowledge gained to predict the outcome in certain situations or with certain parameters.

4. Reported Methods of Break-In

The break-in process includes the gradual electrochemical activation of the stack, gas diffusion, water management and thermal stabilisation, which can be influenced by various factors such as the stack design, materials, operating conditions and test protocols.[9,198] Many advanced methods have been presented in the literature to shorten or otherwise optimise PEMFC, such as lowering the cost by reducing H_2 or energy consumption.[198–199] Most of these studies have been conducted at laboratory scale, which is far from industrial scale in terms of application. Therefore, a simple transfer of these methods is basically impossible. In this section, we will try to bridge the gap between these two worlds by introducing the basic concepts of these methods. By extracting the knowledge from these studies, we aim to highlight some interesting concepts/parameter correlations for possible industrial application.

There are many different break-in methods that can be categorised into two broad groups: online (*in-situ*, hot-break-in) and offline (*ex-situ*, pre-treatment, cold-break-in).[142] The online group includes the more traditional methods such as current/potential control or the various modifications of these methods. It essentially includes all methods in which break-in is performed on a fully assembled stack connected to an activation bench. Offline methods, on the other hand, aim to perform break-in in full or at least partially before the stack is connected to the activation bench and the current/potential controlled protocol is started. These methods are extremely interesting as they could limit or even eliminate the use of the huge activation bench.[200] In the following chapter, we will analyse each concept in terms of what the basic process is, the motivation behind it, which parameters are manipulated, which mechanisms are affected and how. Firstly, we will focus on the online methods, starting with the basic methods, then moving on to the advanced/modified methods and finally continuing with the offline methods.

4.1. Online Break-In Methods

The industry-standard break-in procedure consists of connecting the PEMFC stack to the activation bench and use voltage/current regulation to achieve maximum efficiency.[11] The usual procedure consists of 3 main steps: an initial start-up where the voltage is maintained ("warm-up" phase), an online conditioning ("break-in" phase) and diagnostics.[36] The online break-in procedures differ from each other in that they vary different current steps, ramp types, the number of cycles and the times of the individual stages. Over time, these procedures have become even more differentiated by changing many other parameters such as T, RH, stoichiometry and reactant flow.[36,201]

The most primitive type of break-in consists of simply starting up the FC. This type of break-in is far from ideal as it is time consuming and may trigger some degradation processes.[202] To make break-in feasible in this way, the concept at elevating T and p was introduced. Methods following this concept were presented by Qi et al.[203] (2002; ~2 h) by Qi et al.[204] (2003; ~2 h). The concept of this approach is that an increase in T and p favours the electrochemical reactions and thus accelerates the conditioning processes.

The voltage/current controlled methods are generally based on the following basic principles: Voltage cycling, constant voltage hold, and constant current hold.[19,205–206] These methods are known to be simple to use but time consuming. Voltage cycling protocols usually include several different steps/voltage points, which are then run through several times in the same order. Voltage cycling protocols can also consist of **voltage scans** (Figure 10), which are more common in half-cell measurements and less common in PEMFC stack break-in protocols.[207] When cycling in the range of 0.90 to 0.60 V under O_2, the cathode catalyst surface undergoes an oxidation/reduction process in parallel with the cycling of the generated water. This process changes the catalyst surface, more precisely by oxidation, making the carbon support hydrophilic, which leads to hydration of the ionomer. At high voltage differences, i.e. more than 0.6 V, the oxidation reaction leads to a reorganisation of the catalyst, reportedly resulting in increased TPB,[19] but the voltage windows should be as narrow as

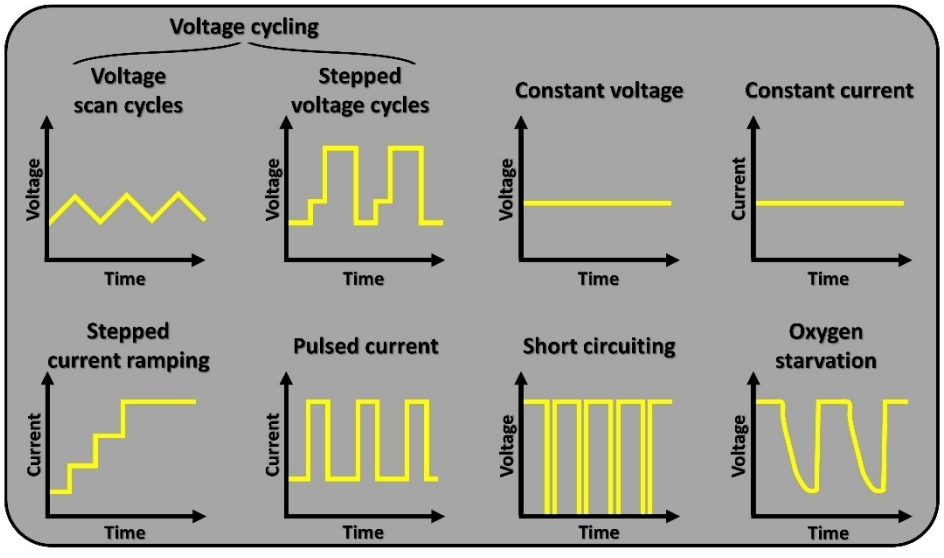

Figure 10. Compilation of primary online break-in methods.

possible, otherwise the break-in may damage the FC.[159,208] The concept of voltage scans was reported by Irmawati et al.[207] (2015), where the voltage was held at 0.6 V and scanned between OCV and 0.3 V after 1 h. It is hypothesised that the ability to scan the voltage slows the recovery of water content in the interface between the Pt ionomer and the membrane, which serves as a precautionary measure to prevent excessive swelling of the membrane. The scanning voltage can also pose a degradation risk, more specifically it can generate metallic cations. This process can also reduce the H^+ conductivity of the ionomer and alter the electroosmotic drag.

Break-in with voltage cycles can also be performed by **voltage steps**, also known as voltage pulsing, (Figure 10), many different protocols have been described by Schrooten et al.[209] (2005; ~5 h), Weng et al.[210] (2007; ~6 h), Stanis et al.[211] (2008; ~16 h), Asghari et al.[212] (2010; ~6 h), Zhang et al.[213] (2010; ~6 h), Yang et al.[214] (2010; ~6 h), Jang et al.[215] (2011; ~7 h) Silva et al.[216] (2012; ~9 h), Rapaport et al.[205] (2015; ~80–90 min), Baricci et al.[217] (2018; ~6 h) and Song et al.[40] (2021; ~4 h). The use of many different voltage steps has been presented, with 0.6 V being the most commonly used. The concept essentially revolves around manipulating the responses with specific voltage pulses/holds to guide the break-in towards optimal activation. Commonly used voltage points for break-in process are 0.6 V, 0.4 V and the OCV; 0.2 V, 0.8 V and 1.0 V are also used somewhat less frequently. The 0.6 V hold is used to initiate moderate electrochemical activity without significantly damaging the catalyst or the membrane. The 0.4 V hold is used to increase the rate of electrochemical activity. This lower voltage accelerates the reduction and oxidation cycles of the catalyst. The increased activity at this voltage also helps to remove impurities. The OCV hold is used to stabilise the components of the fuel cell and balance the system without any current draw. With OCV, the fuel cell is not under load, allowing the mechanical stresses in the MEA to dissipate. This phase is crucial for the hydration of the membrane and for the diffusion of gases and water within the cell. OCV hold ensures that the membrane remains well hydrated and that all localised stresses are relieved before further cycling. However, at the high potential as OCV, oxidation of Pt surface is promoted. To summarise, higher voltages induce Pt oxidation but also relax the PEMFC and mitigate degradation, while lower voltages increase the activation rate and increase the risk of degradation.[114]

A modified method that includes RH cycling and increased T in addition to voltage cycling was shown in the study by Kabir et al.[36] (2019; ~1 h). The concept involves an interaction between voltage (0.6–0.9 V) and RH (32–100 %) at elevated T (80 °C). Elevated T increases the kinetics and accelerates the conditioning mechanisms, but also increases the hydrophobicity of the CL. On the other hand, high RH leads to a higher amount of present water, which influences the rearrangement of the ionomer and increases the hydrophilicity. A cyclical change in RH allows hydration to be controlled, which helps to prevent flooding and regulate the rinsing out of impurities. It is also used to influence Pt dissolution and redeposition, with the possibility of mitigating it at high voltages.[110]

The second basic principle of voltage/current controlled methods is **constant voltage** (Figure 10). This concept is based on only one voltage step (constant voltage hold) during the entire break-in, optionally at elevated T and different RH values. Methods following this concept have been presented by Kim et al.[218] (2006; ~4 h), Guilminot et al.[219] (2007; ~24 h), Jung et al.[220] (2007; ~4 h), Sethuraman et al.[221] (2008; ~8–10 h), Yan et al.[222] (2011; ~24 h), Du et al.[223] (2011; ~12 h), Francia et al.[224] (2011; ~8 h), Jung et al.[225] (2012; ~6–10 h), Yuan et al.[13] (2012; ~2 h), Zhiani et al.[200] (2013; ~12 h), Zhiani et al.[226] (2013; ~9 h), Fu et al.[227] (2014; ~4 h), Park et al.[228] (2015; ~48 h), Zhiani et al.[20] (2016; ~4 h), Zhiani et al.[229] (2017; ~24 h), Taghiabadi et al.[230] (2019), Kim et al.[19] (2020; ~2 h) and Song et al.[231] (2021; ~4 h). The use of a constant voltage approach avoids potential degradation compared to voltage cycling and therefore creates a more controlled environment, but at the cost of lower conditioning effectiveness.[111]

The last of the three principles is **constant current** (Figure 10). In this case, the voltage is regulated by computer so that the desired constant current is achieved. The current is maintained at the same value during the break-in, optionally at an elevated T. This concept has been used by Hsu et al.[232] (1982, ~5 h), Haug et al.[233] (2002; ~4 h), Hou et al.[234] (2007; ~30 min), Bi et al.[235] (2007; ~25 h), Xie et al.[236] (2008; ~6 h), Shan et al.[237] (2010; ~7–10 h), Molla et al.[238] (2011), Yoon et al. (2011; ~15 h), Hou et al.[239] (2011; ~5 h), Rao et al.[240] (2011; ~4 h), Shyu et al.[206] (2011; ~2 h), Zhiani et al.[200] (2013; ~19 h), Kim et al.[19] (2020; ~3 h), Song et al.[231] (2021; ~21 h). The concept of constant current can also consist of merely one constant current value, but in practise the current is usually ramped in steps. In this way, the FC is gradually brought to the desired constant current hold in order to condition it more gently. The main effect of this concept is seen in hydration, while the reduction of surface oxides is not given as much attention as in constant voltage methods. Constant current provides stable, controlled conditions, similar to constant current. The current densities used are 0.1–0.5 A/cm^2 and 1–2 A/cm^2 for high current density hold. Normally, the current is gradually increased due to the initial poor ionic conductivity of PEMFC. The higher the current density, the faster the kinetics and the higher the water and heat generation.

If you work with a constant current for a long time, the voltage can gradually drop. Therefore, countermeasures known

as **voltage recovery** must be taken. It has been described by Uribe et al.[241] (2002), Zhang et al.[242] (2011), Zhang et al.[113] (2012), Rapaport et al.[205] (2015) and Kabir et al.[36] (2019). The principle involves a short voltage drop that restores the recoverable decomposition or rather causes the removal of sulphate, Pt oxides, hydroxides and other anion species. Similar to other method concepts, the kinetics of constant current methods can be enhanced by the addition of elevated T.

Building on the idea of current regulation, the so-called **pulsed current** method (Figure 10) was demonstrated in another case reported by Galistkaya et al.[243] (2018; ~3 h), Wang et al.[244] (2020; ~1 h) and Wang et al.[245] (2021; ~1 h). This type of method has a higher conditioning efficiency, although it can lead to PEMFC degradation if applied improperly/prolonged. In this approach, short pulses with high current density are delivered to the PEMFC. By introducing pauses between the current holds, this concept aims to improve the management of excess water and heat to avoid flooding and high local T that could trigger degradation mechanisms. Compared to constant current and short circuit methods, the pulsed current concept achieves a fast break-in process with less negative impact on the PEMFC.

The concept of **short-circuiting** (Figure 10) is in a way a modification of high-current pulsing. The concept is based on exposing the PEMFC to short short-circuit intervals (~100–200 ms). These methods have an even higher conditioning efficiency, but also an even higher risk of degradation. Application in practise has been reported by Gupta et al.[246] (2017; ~20 min), Trogadas et al.[44] (2020) and Zhang et al.[247] (2021). By applying a short circuit, the voltage drops to almost zero and a high current is reached. This high current state aims to remove oxides and other adsorbed species from the Pt surface and generate water, hydrating the membrane and ionomer, similar to the pulsed current methods. In contrast to pulsed current, short-circuiting generates a large uncontrolled current, which entails a higher activation rate and a higher risk of degradation. Therefore, short-circuiting can be beneficial to a certain extent, but prolonging it can lead to degradation rather than activation. Compared to OCV, for example, the degradation rate is 3x higher,.[247]

In addition to the standard methods, there are also many different modified methods that are built upon voltage/current control, such as carbon monoxide (CO) stripping, cathode starvation, hydrogen pump, reverse flow, etc. The first advanced method is **CO stripping**, which is generally used as a colloquial term for analytical measurement with TF-RDE - CO electro-oxidation. The concept has been extrapolated to the case of break-in, where the catalyst is poisoned with CO and then oxidised, or rather "stripped", to clean the catalyst surface. The application of this concept to PEMFC was demonstrated by Xu et al.[248] (2006; ~2 h). The concept consists of 2 parts: Adsorption and electrooxidation of CO. First, the voltage at the cathode is set to 0.5 V to promote CO adsorption, and then it is scanned to 1 V as CO electro-oxidation occurs at about 0.76 V. In the reported study, the break-in achieved 29% higher maximum performance than the reference break-in (2 h operation at high T and p). The disadvantages are similar to break-in by voltage scanning and also the need to completely remove/clean all CO residues.

One of more interesting concepts is so called **hydrogen pump, which** is based on the concept of H_2 evolution at the cathode. These methods are generally known to be more economical in gas consumption despite high conditioning efficiency. Examples have been shown by Jia et al.[249] (2005), He et al.[250] (2004; ~30 min), Zhang et al.[199] (2018; ~4–6 h), Toyota et al.[251] (2019), Dai et al.[252] (2023; ~30 min), Pei et al.[198] (2024; ~40 min). The basic concept of these methods is the transfer/pumping of H_2 to the cathode via a membrane (Figure 11). In contrary to normal operation, at the cathode compartment, either the inlet can be closed and the outlet opened, or the outlet of the anode compartment is connected to the cathode inlet. With an external power source, H_2 can oxidise at the cathode, traverse membrane and be reduced back to H_2 at the cathode via the known hydrogen evolution reaction (HER). This type of break-in leads to reducing conditions at the cathode, whereby the catalyst surface can be cleaned of Pt oxides. H_2 generation at the surface of the catalyst particles also has the potential to alter the porosity and tortuosity of the CL. This type of break-in can reduce the cost of spent H_2 as it is theoretically only transported through the membrane.

The most widespread method seems to be **oxygen starvation** (Figure 10), which serves as advanced version of hydrogen pump. Many names have appeared in the literature, e.g. air braking, air break method, cathode oxygen depletion, cathode starvation, intermittent oxygen starvation, air starvation, etc.,[40,49,201,231,253–254] but the concept of break-in remains the same: O_2 is removed from the cathode in many cycles. The PEMFC, starts its operation under H_2/O_2, then the current is kept constant as the supply of cathode gas is temporarily interrupted. When the voltage of the cell drops, the O_2 supply is resumed.[201] The concept is basically a combination of current cycling and the principle of H_2 pumping, resulting in methods with high conditioning efficiency. The concept was introduced in practise by Voss et al.[255] (2003; ~1 h), Eickes et al.[256] (2006; ~2 h), Gerard et al.[253] (2010), Balogun et al.[201] (2020; ~40 min), Song et al.[231] (2021; ~2 h), Su et al.[254] (2022), Yang et al.[49] (2022; ~35 min). The concept of O_2 -starvation serves as a modification of the H_2 pump. In the first part of the concept, the cell is operated with a sufficient amount of both reactants, producing water. It is followed by operation with an insufficient supply of O_2, the H^+ from the anode is reduced at the cathode, which

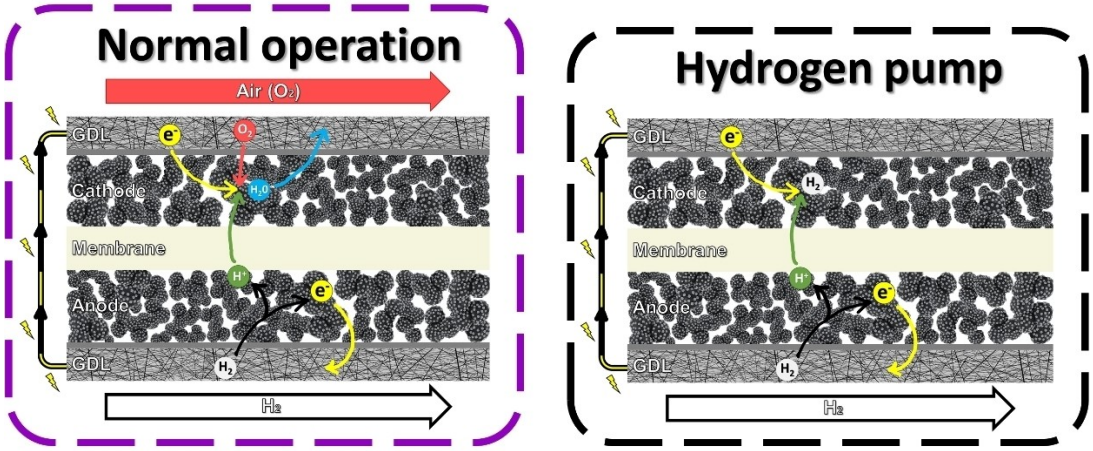

Figure 11. Concept of Normal operation on the left and Hydrogen pump on the right.

corresponds to the concept of the H_2 pump. Accordingly, this crossover improves the H^+ conductivity within the CL and facilitates the reduction of Pt oxides and hydroxides by creating reducing conditions at the cathode. Similar to the H_2 pump, the generation of H_2 can also alter the porosity and tortuosity of the CL. In contrast to the H_2 pump, the O_2 starvation prior to this process created water on the cathode, which is then pulled into the counter current by H^+ (Figure 12). Implementing O_2-starvation break-in also leads to increased porosity. The method is reportedly applicable to

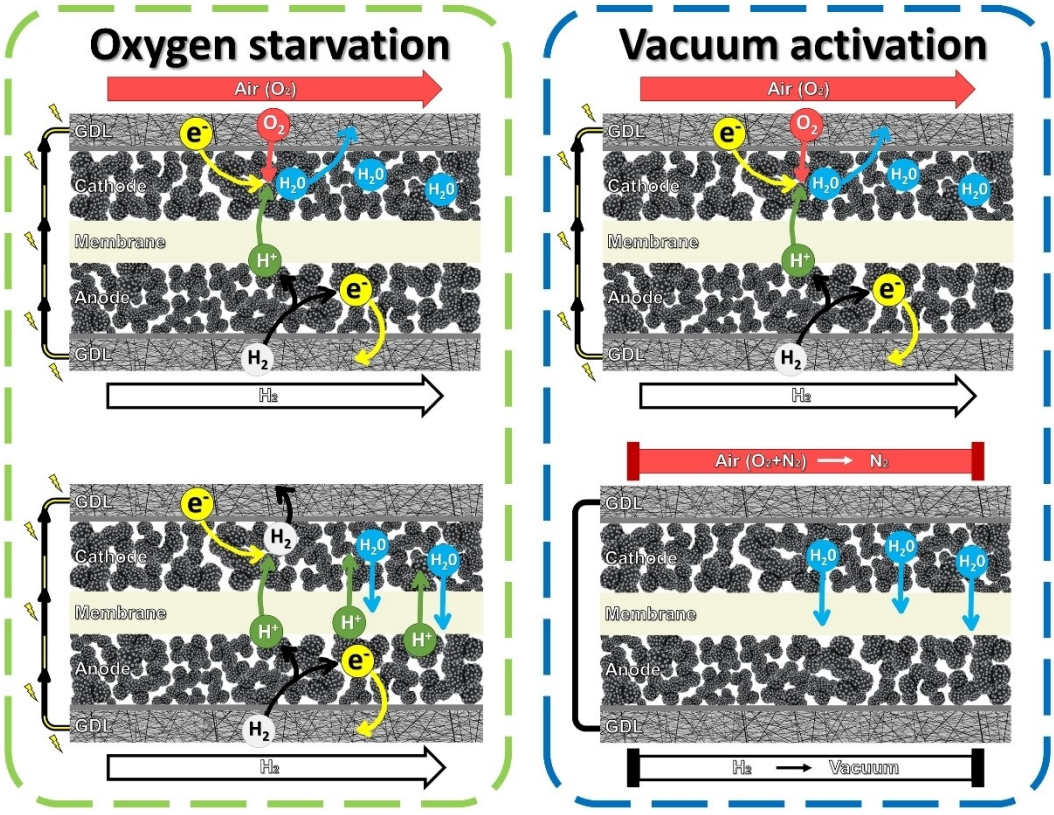

Figure 12. Concept of Oxygen starvation on the left and Vacuum activation on the right.

PEMFCs made of different materials, e.g. catalyst type and loading, GDL type and thickness, MEAs with different active areas, etc.[49] With prolonged conditioning by cathode starvation, the ECSA of the cathode catalyst decreases and the average size of the Pt particles increases.[257] Reportedly, O_2 starvation of 100 s is optimal, or rather, without damaging the PEMFC.[254] While the conditions of O_2-starvation can lead to conditioning of the PEMFC, H_2 starvation only leads to degradation, such as carbon corrosion.[258]

Another unique method presented by Yang et al.[88] (2016; ~30 min), revolves around the so-called **vacuum activation**. The method starts with maintaining a high current density to generate water. Subsequently, the current density is kept low to slowly decrease the voltage to 0.4 V without supplying H_2 and air, and in the last step, air is added to the anode or cathode. Thus, no H_2 and air are supplied to the stack during vacuum activation, so that the remaining H_2 and O_2 molecules in the stack would be gradually consumed. As a result, the partial p at the anode decreases significantly compared to that at the cathode, which is mainly due to the partial p of the remaining N_2 gas from the air. This p difference facilitates the transport of water from the cathode to the anode through the polymer membrane (Figure 12).

The next approach is based on **temperature cycling**. It was described by Kagami et al.[259] (2005), Yang et al.[260] (2011; ~3 h), Debe et al.[261] (2012; ~8 h) and Bezmalinović et al.[262] (2014; ~40 min). The concept involves humidification of the PEMFC at elevated T, followed by a sudden drop in T. This leads to condensation of water in the membrane and accelerates membrane hydration. For example, the PEMFC is operated at elevated T with humidified gaseous reactant to maximise humidification. Subsequently, the operation is stopped, purged dry and the T is lowered to a value below zero, causing the moisture in the PEM to condense (Figure 13).[259] The presence of liquid water in the CL maintains close contact with the polymer, which is preferable to supersaturated gases flowing through the channels, as the water condenses primarily within the flow field channels.[262] When the polymer comes into contact with liquid water instead of vapour, this leads to a change in its surface skin, resulting in an increase in hydrophilicity.[76] On the other hand, frequent cycling can have a negative effect on cell lifetime.[262]

Following with an example of break-in concept where the **reverse flow** is applied, as reported by Park et al.[263] (2021; ~68 min). In order to minimise the different effect of conditioning at the inlet and outlet due to the concentration gradient, a new concept of break-in has been developed. Essentially, the direction of the reactant flow is changed repeatedly. Thus, the O_2 reduction and H_2 reforming zones alternate, resulting in a more uniform desorption of oxides and impurities (Figure 13). As the cathode flow is reversed during stack operation, there is also a temporary O2 depletion, which triggers the conditioning mechanisms associated with cathode depletion mentioned above.

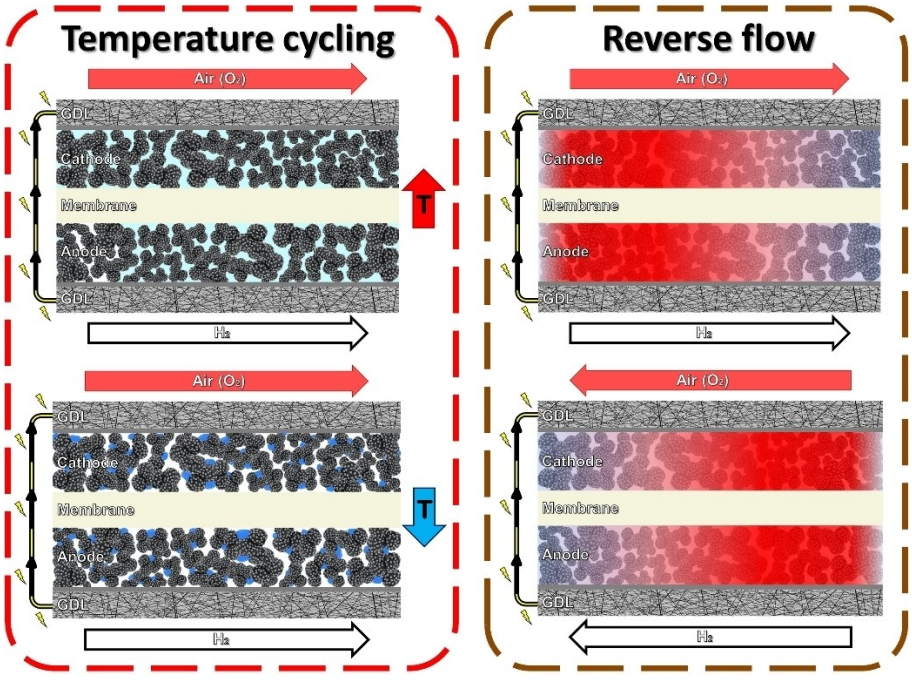

Figure 13. Concept of Temperature cycling on the left and Reverse flow on the right.

Finally, methods with **combined multiple steps** are also presented. Xu et al.[264] (2006) presented a combined concept of conditioning PEMFC at elevated T and p, followed by H_2 pumping and final CO stripping. It combined the positive features of hydration-focussed conditioning and catalyst surface cleaning methods by H_2 pumping and CO stripping, which further improved the performance of PEMFC. Choo et al.[95] (2019; ~20 min) combine the pulsed current concept with H_2 pumping. They apply a high current pulse to the PEMFC stack and pump H_2 to the cathode during the turn-off process. By extending the duration of the high current voltammetry pulse through a gradual sweep of the pulse potential, the formation of an ionic pathway is facilitated by the reorganisation of sulphonic acid groups, promoting the wetting of the PEM and ionomer. Before switching off, the voltage drops to 0 V to reach an O_2-free state. This enables the creation of a reduction atmosphere with an H_2 pump and thus the reduction of surface oxides. Hu et al.[265] (2020; ~3 h) have demonstrated a three-step break-in concept similar to the T-cycle: a low RH step, a supersaturated humidity step, and another low RH step. The first step focuses on creating a Pt ionomer interface within the CL that is free from the constraints of gas transport. The second step aims to increase the water content within the CL. And the third step aims to optimise the performance of the CL. As the first two steps aim to maximise the water content, the third step is carried out at a relatively low RH to prevent water flooding. The first two steps also contribute to conditioning by pore-forming mechanisms; the first step induces the mechanism of pore hollowing, while the second step stimulates pore swelling. Pei et al.[198] (2024; ~40 min) chose a different approach to combine multiple break-in concepts. A combination of H_2 pumping and boundary flow activation with trapped air was presented. Thus, it is a combination of a strongly reducing atmosphere and a water supply from the cathode to the anode with the H_2 pumping concept and flooding-like conditions at the cathode due to limited gas purging and a reducing atmosphere due to the low potential with the concept of current-limited activation with confined air.

Although many different interesting concepts and modifications of online break-in have been reported, they still require a significant amount of time on the activation bench, which buffers the production line. To further reduce or even eliminate this time, we will explore intriguing offline approaches in the following subsection.

4.2. Offline Break-In Methods

In contrast to online break-in, offline methods offer a distinct approach for conditioning PEMFC stacks. These methods are characterised by the fact that they can condition the PEMFC components independently of the operating system. Offline methods typically involve chemical, thermal or mechanical treatments to achieve the desired performance prior to installation in the stack. In this section, the various offline methods described in the literature, their process concept and the reasoning behind them are presented to provide a comprehensive understanding of their role in improving the efficiency and longevity of PEMFCs.

The first method on the list involves the injection of **H_2-infused water droplets** as described by Choo et al.[266] (2014; ~1 −5 days). During assembly, H_2-containing droplets are injected into both the anode and the cathode at high T. The stack is then sealed and allowed to rest at RT. H_2 creates a reducing environment on the cathode, which reduces the surface oxides formed on the surface of the Pt catalyst. Dissolved Pt ions can redeposit, creating a vacuum. According to the reference, 50 % of the break-in is achieved with a 1-day rest period, but an even higher level, namely 83 %, is achieved with a 5-day rest period. By infusing H_2-containing droplets on the cathode and O_2-containing droplets on the anode and resting the sealed PEMFC stack, 100 % break-in is possible. In this way, the oxides are reduced, similar to before. The droplets easily penetrate the membrane and ionomer due to the vacuum created by the transition of H_2 and O_2 during storage in the PEMFC stack and improve the wetting properties.

Zhiani et al.[267] (2014; ~1 h). reported a method using **ultrasonic waves**. The concept is that the PEMFC is treated with ultrasonic waves before it is conditioned online. According to the source, a 1-hour preconditioning in an ultrasonic bath at 60 °C removes the pre-existing impurities, increases the size and volume of the pores and reduces the online conditioning by up to 30 %.

The next concept involves the use of an **acidic solution** to perform an offline break-in, optionally at elevated temperatures or connected to the load. Methods following this practise have been reported by Xu et al.[268] (2003; ~10 min), Parrondo et al.[39] (2007), Palanichamy et al.[269] (2008; ~4–12 h), Barrio et al.[270] (2009) and Cho et al.[169] (2010; ~1 h). The concept may involve only immersion in acid, but it may also involve elevated T (up to 100 °C). The acid used is usually H_2SO_4, but the use of peracetic acid (PAA) and HNO_3 in combination with H_2O_2 has also been reported. Exposure to acids and heat changes the physico-chemical properties of the polymer matrix and increases its ability to absorb water, making humidification unnecessary. The hydrophilicity or wettability of the surface is also improved, which is due to the increase in the O_2 atom ratio. The process also improves the porosity and tortuosity of the CL. Performance is reported to improve by around 47 % compared to untreated MEA.

Following with methods that involve **boiling or steaming** PEMFC. The concept is relatively simple as it only requires boiling water or steam. The concept was introduced by Qi et

al[236] (2002; ~10 min), Anderson et al.[10] (2002; ~10 min), Anderson et al.[271] (2009; ~10–25 min), Silva et al.[272] (2012) and Zhiani et al.[229] (2017; ~2,5 h). The treatment improves the water holding capacity within the CL, eliminating the need for air humidification. The proposed mechanism is that the treatment improves the surface wettability and H^+ conductivity of the carbon particles while increasing the porosity and tortuosity of the CL. The hot water/steam treatment opens certain blocked areas and makes them accessible. Boiling the PEMFC also leads to an increase in the distance between the polymer domains and a decrease in crystallinity, which promotes swelling and water uptake. Boiling/steaming has been reported to increase the performance of PEMFC by up to 40%. In the study by Zhiani et al.,[229] the steaming concept was presented slightly differently. Instead of steaming the electrodes before assembling the PEMFC, vapour is injected on both sides of the PEMFC in this variant. This approach offers advantages over steaming/boiling electrodes, as the vapour flows through the flow field channels and then condenses in the various layers of the MEA. This leads to increased water uptake within the membrane, which contributes to improved performance. Improved mass transfer within the MEA is achieved either by removing unbound particles or by creating new transport pathways from the CL surface.

The last offline method was presented by Yang et al.[88] (2016; ~2 h) and Yang et al.[35] (2017; ~24 h) and revolves around **soaking** the entire stack in **DI water**. The concept is to immerse/fill the air-breathing PEMFC stack in DI water until all the voids are filled with water and then let it rest for a certain time. After 24 hours of preconditioning, Yang et al.[35] achieved peak performance after only 1 hour of break-in time (constant current at 0.65 V) compared to the 24-hour conventional activation method. Yang et al.[88] succeeded in accelerating the break-in time to 30 minutes with only 2 hours of preconditioning with hot DI water. Immersion in DI water increases the H^+ conductivity due to the phase separation between hydrophilic and hydrophobic regions, which is due to the swelling of the PEM. It also improves O_2 transport due to phase separation within the ionomer near the Pt electrocatalyst. The described concept is highly interesting for the industry as it can be relatively easily integrated into the production line and significantly reduces the time on the activation bench.

5. Conclusion

PEMFCs are already recognised as mature technology, However, there remains significant potential for further optimization and improvement, particularly in the context of large-scale industrial production and the extension of stack lifetimes. Research groups worldwide are exploring unique approaches to enhance different components of PEMFCs. As a result, a standardized, simple, and quick procedure or a "one-size-fits-all" solution for the break-in process is not feasible. Understanding the key aspects of this break-in process, as well as the necessary actions at the micro- and nanoscale, is crucial for producing a well-conditioned PEMFC product. A customized break-in process tailored to the specific components and operating conditions of a particular PEMFC can help ensure efficient and effective conditioning. This leads to shorter process durations, reduced operating costs, optimal performance, and prolonged lifespan of the stacks.

Our literature review aims to clarify the complexities underlying the break-in process and serves as a foundational reference for future research. It discusses potential mechanisms that occur during conditioning, presents methods for analyzing these mechanisms, and offers tools for investigation and monitoring. Furthermore, the insights gained from this review could be integrated into multiscale modeling efforts, enhancing the understanding of the break-in process and the overall functionality of PEMFCs.

A key contribution of this article is the compilation of previously reported break-in methods. We have identified the fundamental concepts underlying these methods, their differences, and how their unique characteristics influence the break-in process. By laying this foundation, we aim to facilitate future work on PEMFC break-in and accelerate the commercialization of optimized break-in procedures. This will spark new questions, such as how faster and more affordable break-in protocols affect the lifetime of MEAs, the impact of GDLs, and how long a cell can be out of service before another break-in becomes necessary–all of which will need to be addressed. This focus on refining break-in processes not only supports the feasibility of large-scale industrial production but also contributes to the goal of extending the operational life of PEMFC stacks.

Author Contributions

Mitja Kostelec: writing – original draft, writing – review and editing, design and preparation of schemes. Matija Gatalo: Resources, writing – review and editing, supervision. Nejc Hodnik: resources, writing – review and editing, supervision.

Acknowledgements

The authors would like to acknowledge the Slovenian research agency (ARRS) programs P2–0393 and I0–0003; the projects NC-0016, N2–0257 and J7–4637; EIC Transition project ENABLER (grant agreement ID: 101112991); European Research Council (ERC) Starting Grant 123STABLE (grant agreement ID: 852208); and K. M. acknowledges EKPO Fuel Cell Technologies GmbH for funding.

References

[1] L. Zhang, S.-R. Chae, Z. Hendren, J.-S. Park, M. R. Wiesner, *Chem. Eng. J.* **2012**, *204–206*, 87–97.
[2] O. Gröger, H. A. Gasteiger, J.-P. Suchsland, *J. Electrochem. Soc.* **2015**, *162*, A2605–A2622.
[3] P. Tech, "PowerUp Energy Technology," can be found under https://powerup-tech.com/, (accessed March 15, 2024).
[4] L. Fan, Z. Tu, S. H. Chan, *Energy Reports* **2021**, *7*, 8421–8446.
[5] J. P. Braaten, X. Xu, Y. Cai, A. Kongkanand, S. Litster, *J. Electrochem. Soc.* **2019**, *166*, F1337–F1343.
[6] K. Jiao, J. Xuan, Q. Du, Z. Bao, B. Xie, B. Wang, Y. Zhao, L. Fan, H. Wang, Z. Hou, S. Huo, N. P. Brandon, Y. Yin, M. D. Guiver, *Nature* **2021**, *595*, 361–369.
[7] M. M. Tellez-Cruz, J. Escorihuela, O. Solorza-Feria, V. Compañ, *Polymers (Basel).* **2021**, *13*, 3064.
[8] J. Zhang, H. Zhang, J. Wu, J. Zhang, in *Pem Fuel Cell Test. Diagnosis*, Elsevier, **2013**, pp. 43–80.
[9] M. S. Habib, P. Arefin, M. A. Salam, K. Ahmed, M. S. Uddin, T. Hossain, N. Papri, T. Islam, *Mater. Sci. Res. India* **2021**, *18*, 217–234.
[10] Z. Qi, A. Kaufman, *J. Power Sources* **2002**, *109*, 227–229.
[11] F. Van Der Linden, E. Pahon, S. Morando, D. Bouquain, *J. Power Sources* **2023**, *575*, 233168.
[12] M. Gatalo, A. M. Bonastre, L. J. Moriau, H. Burdett, F. Ruiz-Zepeda, E. Hughes, A. Hodgkinson, M. Šala, L. Pavko, M. Bele, N. Hodnik, J. Sharman, M. Gaberšček, *ACS Appl. Energ. Mater.* **2022**, *5*, 8862–8877.
[13] X.-Z. Yuan, J. C. Sun, H. Wang, H. Li, *J. Power Sources* **2012**, *205*, 340–344.
[14] E. B. Agyekum, J. D. Ampah, T. Wilberforce, S. Afrane, C. Nutakor, *Membranes* **2022**, *12*, 1103.
[15] "Is the cost of fuel cells a major problem?," can be found under https://auto.howstuffworks.com/fuel-efficiency/alternative-fuels/cost-of-fuel-cells-a-major-problem.htm, (accessed March 17, 2024).
[16] Y. Wang, Y. Pang, H. Xu, A. Martinez, K. S. Chen, *Energy Environ. Sci.* **2022**, *15*, 2288–2328.
[17] "Why are the Prices of Fuel Cells Dropping?," can be found under https://www.horizoneducational.com/why-are-the-prices-of-fuel-cells-dropping/t1422?currency=usd, (accessed March 17, 2024).
[18] G. Farré, S. Gómez-Galera, S. Naqvi, C. Bai, G. Sanahuja, D. Yuan, U. Zorrilla-López, L. Codony, E. Rojas, M. Fibla, R. Twyman, T. Capell, P. Christou, C. Zhu, *Encyclopedia of Sustainability Science and Technology*, Springer New York, New York, NY, NY, **2012**.
[19] M. S. Kim, J. H. Song, D. K. Kim, *Energies* **2020**, *13*, 2831.
[20] M. Zhiani, S. Majidi, V. B. Silva, H. Gharibi, *Energy* **2016**, *97*, 560–567.
[21] "How Hydrogen Combustion Engines Will Challenge The EV Market At Its Core," can be found under https://www.topspeed.com/how-hydrogen-combustion-engines-challenge-evs/, (accessed March 20, 2024).
[22] "The Future of Fuel Cells," can be found under https://www.horizoneducational.com/the-future-of-fuel-cells/t1426, (accessed March 20, 2024).
[23] "The End of Combustion and the Post-fossil Era," can be found under https://media.smart.com/eu/the-end-of-combustion-and-the-post-fossil-era/#, (accessed March 20, 2024).
[24] "What will happen to internal combustion engine cars after 2025?," can be found under https://knaufautomotive.com/what-will-happen-to-internal-combustion-engine-cars-after-2025/), (accessed March 20, 2024).
[25] "Fit for 55: deal on charging and fuelling stations for alternative fuels," can be found under https://www.europarl.europa.eu/news/en/press-room/20230327IPR78504/fit-for-55-deal-on-charging-and-fuelling-stations-for-alternative-fuels, (accessed March 20, 2024).
[26] "State Aid: Commission approves up to €5.4 billion of public support by fifteen Member States for an Important Project of Common European Interest in the hydrogen technology value chain," can be found under https://ec.europa.eu/commission/presscorner/detail/en/IP_22_4544, (accessed March 20, 2024).
[27] "Central Queensland hydrogen (CQ–H2) Project," can be found under https://www.stanwell.com/energy-assets/new-energy-initiatives/stanwell-hydrogen-project/stanwell-hydrogen-project/, (accessed March 230, 2024).
[28] X.-Z. Yuan, S. Zhang, J. C. Sun, H. Wang, *J. Power Sources* **2011**, *196*, 9097–9106.
[29] K. Christmann, K. A. Friedrich, N. Zamel, *Prog. Energy Combust. Sci.* **2021**, *85*, 100924.
[30] S. S. Kocha, B. G. Pollet, *Curr. Opin. Electrochem.* **2022**, *31*, 100843.
[31] P. Pei, X. Fu, Z. Zhu, P. Ren, D. Chen, *Int. J. Hydrogen Energy* **2022**, *47*, 24897–24915.
[32] M. Ma, L. Shen, Z. Zhao, P. Guo, J. Liu, B. Xu, Z. Zhang, Y. Zhang, L. Zhao, Z. Wang, *eScience* **2024**, 100254.
[33] R. O'Hayre, S.-W. Cha, W. Colella, F. B. Prinz, *Fuel Cell Fundamentals*, John Wiley & Sons, Inc, Hoboken, NJ, USA, NJ, USA, **2016**.
[34] A. Atkinson, A. J. Marquis, in *Handb. Fuel Cells*, Wiley, **2010**.
[35] S. Y. Yang, D.-J. Seo, M.-R. Kim, W.-Y. Choi, Y.-G. Yoon, M.-H. Seo, B.-J. Kim, C.-Y. Jung, H. Kim, B. Han, T.-Y. Kim, *Int. J. Hydrogen Energy* **2017**, *42*, 16288–16293.
[36] S. Kabir, D. J. Myers, N. Kariuki, J. Park, G. Wang, A. Baker, N. Macauley, R. Mukundan, K. L. More, K. C. Neyerlin, *ACS Appl. Mater. Interfaces* **2019**, *11*, 45016–45030.
[37] Y. Yurko, L. Elbaz, *Electrochim. Acta* **2021**, *389*, 138676.
[38] J. P. Meyers, **2009**, pp. 19–39.
[39] J. Parrondo, M. Ortueta, F. Mijangos, *Braz. J. Chem. Eng.* **2007**, *24*, 411–419.
[40] J. hee Song, M. soo Kim, Y. rim Kang, D. kyu Kim, *J. Energy Storage* **2021**, *44*, 103338.
[41] Harilal, R. Nayak, P. C. Ghosh, T. Jana, *ACS Appl. Polym. Mater.* **2020**, *2*, 3161–3170.
[42] B. Soleimani, A. H. Asl, B. Khoshandam, K. Hooshyari, *Sci. Rep.* **2023**, *13*, 8238.
[43] T. Tingelöf, J. K. Ihonen, *Int. J. Hydrogen Energy* **2009**, *34*, 6452–6456.

[44] P. Trogadas, J. I. S. Cho, N. Kapil, L. Rasha, A. Corredera, D. J. L. Brett, M.-O. Coppens, *Sustain. Energy Fuels* **2020**, *4*, 5739–5746.
[45] R. Sgarbi, W. Ait Idir, Q. Labarde, M. Mermoux, P. Wu, J. Mainka, J. Dillet, C. Marty, F. Micoud, O. Lottin, M. Chatenet, *Ind. Chem.* **2023**, *1*, 501–515.
[46] J. Mitzel, J. Sanchez-Monreal, D. Garcia-Sanchez, P. Gazdzicki, M. Schulze, F. Häußler, J. Hunger, G. Schlumberger, E. Janicka, M. Mielniczek, L. Gawel, *Fuel Cells* **2020**, *20*, 403–412.
[47] M. Gatalo, L. Moriau, U. Petek, F. Ruiz-Zepeda, M. Šala, M. Grom, T. Galun, P. Jovanovič, A. Pavlišič, M. Bele, N. Hodnik, M. Gaberšček, *Electrochim. Acta* **2019**, *306*, 377–386.
[48] M. Ronovsky, O. Dunseath, T. Hrbek, P. Kus, M. Gatalo, S. Polani, J. Kubat, D. Götz, H. Nedumkulam, A. Satori, E. Petrucco, F. R. Zepeda, N. Hodnik, P. Strasser, A. M. Bonastre, J. Drnec, *ChemRxiv.* **2024**, DOI 10.26434/chemrxiv-2024-g9lx2.
[49] D. Yang, Y. Lan, T. Chu, B. Li, P. Ming, C. Zhang, X. Zhou, *Energy* **2022**, *260*, 125154.
[50] B. Ruiz-Camacho, J. C. Baltazar Vera, A. Medina-Ramírez, R. Fuentes-Ramírez, G. Carreño-Aguilera, *Int. J. Hydrogen Energy* **2017**, *42*, 30364–30373.
[51] T. A. M. Suter, K. Smith, J. Hack, L. Rasha, Z. Rana, G. M. A. Angel, P. R. Shearing, T. S. Miller, D. J. L. Brett, *Adv. Energy Mater.* **2021**, *11*, 2101025.
[52] D. Van Dao, G. Adilbish, T. D. Le, I.-H. Lee, Y.-T. Yu, *RSC Adv.* **2019**, *9*, 15635–15641.
[53] R. Subbaraman, D. Strmcnik, A. P. Paulikas, V. R. Stamenkovic, N. M. Markovic, *ChemPhysChem* **2010**, *11*, 2825–2833.
[54] H. A. Gasteiger, S. S. Kocha, B. Sompalli, F. T. Wagner, *Appl. Catal. B* **2005**, *56*, 9–35.
[55] V. Yarlagadda, M. K. Carpenter, T. E. Moylan, R. S. Kukreja, R. Koestner, W. Gu, L. Thompson, A. Kongkanand, *ACS Energy Lett.* **2018**, *3*, 618–621.
[56] M. Xie, T. Chu, T. Wang, K. Wan, D. Yang, B. Li, P. Ming, C. Zhang, *Membranes* **2021**, *11*, 879.
[57] H. Wang, R. Wang, S. Sui, T. Sun, Y. Yan, S. Du, *Automot. Innov.* **2021**, *4*, 144–164.
[58] A. Kongkanand, M. F. Mathias, *J. Phys. Chem. Lett.* **2016**, *7*, 1127–1137.
[59] D. J. S. Sandbeck, M. Inaba, J. Quinson, J. Bucher, A. Zana, M. Arenz, S. Cherevko, *ACS Appl. Mater. Interfaces* **2020**, *12*, 25718–25727.
[60] D. J. S. Sandbeck, N. M. Secher, F. D. Speck, J. E. Sørensen, J. Kibsgaard, I. Chorkendorff, S. Cherevko, *ACS Catal.* **2020**, *10*, 6281–6290.
[61] W. Chen, C. Cai, S. Li, J. Tan, M. Pan, *Int. J. Hydrogen Energy* **2021**, *46*, 8749–8757.
[62] R. O'Hayre, F. B. Prinz, *J. Electrochem. Soc.* **2004**, *151*, A756.
[63] R. Subbaraman, D. Strmcnik, A. P. Paulikas, V. R. Stamenkovic, N. M. Markovic, *ChemPhysChem* **2010**, *11*, 2825–2833.
[64] N. Zhao, X. Yuan, F. Girard, K. Wang, J. Li, Z. Shi, Z. Xie, *ChemistrySelect* **2019**, *4*, 12649–12655.
[65] A. Chumakov, V. Batalova, Y. Slizhov, in *AIP Conf. Proc.*, **2016**, p. 040004.
[66] D. Han, M. Tsipoaka, S. Shanmugam, *J. Power Sources* **2021**, *496*, 229816.
[67] K. Hongsirikarn, J. G. Goodwin, S. Greenway, S. Creager, *J. Power Sources* **2010**, *195*, 7213–7220.
[68] Nafion, "Powering Fuel Cells with Nafion™ Membranes," (accessed April 10, 2024).
[69] "Aquavion," can be found under https://www.syensqo.com/en/brands/aquivion-ion-conducting-polymers, (accessed April 10, 2024).
[70] "Fumion® polymers and dispersions for electrochemical processes," can be found under https://www.fumatech.com/en/products/fumion/, (accessed April 10, 2024).
[71] "Pemion," can be found under https://ionomr.com/solutions/pemion/, **2024**.
[72] N. Zamel, *J. Power Sources* **2016**, *309*, 141–159.
[73] P. Z. Lin, J. Sun, M. C. Wu, T. S. Zhao, *Int. J. Heat Mass Transfer* **2022**, *195*, 123092.
[74] P. C. Okonkwo, I. Ben Belgacem, W. Emori, P. C. Uzoma, *Int. J. Hydrogen Energy* **2021**, *46*, 27956–27973.
[75] K. Malek, T. Mashio, M. Eikerling, *Electrocatalysis* **2011**, *2*, 141–157.
[76] M. Bass, A. Berman, A. Singh, O. Konovalov, V. Freger, *J. Phys. Chem. B* **2010**, *114*, 3784–3790.
[77] T. Kadyk, R. Hanke-Rauschenbach, K. Sundmacher, *J. Electroanal. Chem.* **2009**, *630*, 19–27.
[78] O. S. Ijaodola, Z. El- Hassan, E. Ogungbemi, F. N. Khatib, T. Wilberforce, J. Thompson, A. G. Olabi, *Energy* **2019**, *179*, 246–267.
[79] L. Shen, M. Ma, Z. Zhao, F. Tu, J. Liu, B. Xu, Y. Zhang, L. Zhao, G. Shao, Z. Wang, *J. Power Sources* **2023**, *575*, 233202.
[80] X. R. Wang, Y. Ma, J. Gao, T. Li, G. Z. Jiang, Z. Y. Sun, *Int. J. Hydrogen Energy* **2021**, *46*, 12206–12229.
[81] M. Capdevila-Cortada, *Nat. Catal.* **2022**, *5*, 969–969.
[82] T. H. Yu, Y. Sha, W.-G. Liu, B. V. Merinov, P. Shirvanian, W. A. Goddard, *J. Am. Chem. Soc.* **2011**, *133*, 19857–19863.
[83] P. Strasser, S. Kühl, *Nano Energy* **2016**, *29*, 166–177.
[84] M. Niu, Y. Gao, Q. Pan, T. Zhang, *Ionics* **2024**, DOI 10.1007/s11581-024-05449-w.
[85] F. D. Coms, H. Liu, J. E. Owejan, *ECS Meet. Abstr.* **2008**, *MA2008–02*, 1057–1057.
[86] W. Olbrich, T. Kadyk, U. Sauter, M. Eikerling, J. Gostick, *Sci. Rep.* **2023**, *13*, 14127.
[87] C. O. Colpan, Y. Nalbant, M. Ercelik, in *Compr. Energy Syst.*, Elsevier, **2018**, pp. 1107–1130.
[88] S. Y. Yang, D.-J. Seo, M.-R. Kim, M. H. Seo, S.-M. Hwang, Y.-M. Jung, B.-J. Kim, Y.-G. Yoon, B. Han, T.-Y. Kim, *J. Power Sources* **2016**, *328*, 75–80.
[89] J. Zhang, S. Shen, in *Book*, **2021**, pp. 167–222.
[90] S. Papasavva, M. Veenstra, J. Waldecker, T. West, *Int. J. Hydrogen Energy* **2021**, *46*, 21136–21150.
[91] S. G. Rinaldo, W. Lee, J. Stumper, M. Eikerling, *Electrocatalysis* **2014**, *5*, 262–272.
[92] D. E. Ramaker, A. Korovina, V. Croze, J. Melke, C. Roth, *Phys. Chem. Chem. Phys.* **2014**, *16*, 13645–13653.

[93] D. W. Kumsa, N. Bhadra, E. M. Hudak, S. C. Kelley, D. F. Untereker, J. T. Mortimer, *J. Neural Eng.* **2016**, *13*, 052001.
[94] S. Prass, J. St-Pierre, M. Klingele, K. A. Friedrich, N. Zamel, *Electrocatalysis* **2021**, *12*, 45–55.
[95] H. S. Choo, *Method of Accelerating Fuel Cell Activation*, US 10, 256, 487 B2, U.S. Patent, **2019**.
[96] M. Khorshidian, M. Sedighi, *Iran. J. Hydrog. Fuel Cell* **2019**, *2*, 91–115.
[97] S. Zhu, X. Hu, M. Shao, *Phys. Chem. Chem. Phys.* **2017**, *19*, 7631–7641.
[98] L. Pavko, M. Gatalo, G. Križan, J. Križan, K. Ehelebe, F. Ruiz-Zepeda, M. Šala, G. Dražić, M. Geuß, P. Kaiser, M. Bele, M. Kostelec, T. Đukić, N. Van de Velde, I. Jerman, S. Cherevko, N. Hodnik, B. Genorio, M. Gaberšček, *ACS Appl. Energ. Mater.* **2021**, *4*, 13819–13829.
[99] A. C. Bhosale, P. C. Ghosh, L. Assaud, *Renewable Sustainable Energy Rev.* **2020**, *133*, 110286.
[100] H. R. Haas, *ECS Meet. Abstr.* **2009**, *MA2009–02*, 1082–1082.
[101] D. J. S. Sandbeck, N. M. Secher, M. Inaba, J. Quinson, J. E. Sørensen, J. Kibsgaard, A. Zana, F. Bizzotto, F. D. Speck, M. T. Y. Paul, A. Dworzak, C. Dosche, M. Oezaslan, I. Chorkendorff, M. Arenz, S. Cherevko, *J. Electrochem. Soc.* **2020**, *167*, 164501.
[102] R. Alink, R. Singh, P. Schneider, K. Christmann, J. Schall, R. Keding, N. Zamel, *Molecules* **2020**, *25*, 1523.
[103] P. C. Okonkwo, O. O. Ige, E. M. Barhoumi, P. C. Uzoma, W. Emori, A. Benamor, A. M. Abdullah, *Int. J. Hydrogen Energy* **2021**, *46*, 15850–15865.
[104] S. Mezzavilla, S. Cherevko, C. Baldizzone, E. Pizzutilo, G. Polymeros, K. J. J. Mayrhofer, *ChemElectroChem* **2016**, *3*, 1524–1536.
[105] J. P. Sabawa, A. S. Bandarenka, *Int. J. Hydrogen Energy* **2021**, *46*, 15951–15964.
[106] M. Schulze, N. Wagner, T. Kaz, K. A. Friedrich, *Electrochim. Acta* **2007**, *52*, 2328–2336.
[107] H.-E. Kim, J. Kwon, H. Lee, *Chem. Sci.* **2022**, *13*, 6782–6795.
[108] J. Schröder, J. Quinson, J. K. Mathiesen, J. J. K. Kirkensgaard, S. Alinejad, V. A. Mints, K. M. Ø Jensen, M. Arenz, *J. Electrochem. Soc.* **2020**, *167*, 134515.
[109] S. Cherevko, N. Kulyk, K. J. J. Mayrhofer, *Nano Energy* **2016**, *29*, 275–298.
[110] C. Takei, K. Kakinuma, K. Kawashima, K. Tashiro, M. Watanabe, M. Uchida, *J. Power Sources* **2016**, *324*, 729–737.
[111] A. A. Topalov, S. Cherevko, A. R. Zeradjanin, J. C. Meier, I. Katsounaros, K. J. J. Mayrhofer, *Chem. Sci.* **2014**, *5*, 631–638.
[112] J. Zhang, Y. Tang, C. Song, J. Zhang, H. Wang, *J. Power Sources* **2006**, *163*, 532–537.
[113] J. Zhang, B. A. Litteer, F. D. Coms, R. Makharia, *J. Electrochem. Soc.* **2012**, *159*, F287–F293.
[114] S. Sugawara, T. Maruyama, Y. Nagahara, S. S. Kocha, K. Shinohra, K. Tsujita, S. Mitsushima, K. Ota, *J. Power Sources* **2009**, *187*, 324–331.
[115] Y. Shao-Horn, W. C. Sheng, S. Chen, P. J. Ferreira, E. F. Holby, D. Morgan, *Top. Catal.* **2007**, *46*, 285–305.
[116] K. J. J. Mayrhofer, J. C. Meier, S. J. Ashton, G. K. H. Wiberg, F. Kraus, M. Hanzlik, M. Arenz, *Electrochem. Commun.* **2008**, *10*, 1144–1147.
[117] Y. Yin, R. Li, F. Bai, W. Zhu, Y. Qin, Y. Chang, J. Zhang, M. D. Guiver, *Electrochem. Commun.* **2019**, *109*, 106590.
[118] T. Kaneko, J. Ooyama, M. Ohki, H. Kanesaka, Y. Yoshimoto, I. Kinefuchi, *Int. J. Heat Mass Transfer* **2023**, *200*, 123491.
[119] V. Čolić, A. S. Bandarenka, *ACS Catal.* **2016**, *6*, 5378–5385.
[120] S. C. Zignani, E. Antolini, E. R. Gonzalez, *J. Power Sources* **2008**, *182*, 83–90.
[121] M. Gummalla, S. Ball, D. Condit, S. Rasouli, K. Yu, P. Ferreira, D. Myers, Z. Yang, *Catalysts* **2015**, *5*, 926–948.
[122] Y. Cai, J. M. Ziegelbauer, A. M. Baker, W. Gu, R. S. Kukreja, A. Kongkanand, M. F. Mathias, R. Mukundan, R. L. Borup, *J. Electrochem. Soc.* **2018**, *165*, F3132–F3138.
[123] C. Lee, X. Wang, J.-K. Peng, A. Katzenberg, R. K. Ahluwalia, A. Kusoglu, S. Komini Babu, J. S. Spendelow, R. Mukundan, R. L. Borup, *ACS Appl. Mater. Interfaces* **2022**, *14*, 35555–35568.
[124] N. Ramaswamy, S. Kumaraguru, K. Jarvis, P. Ferreira, *J. Electrochem. Soc.* **2023**, *170*, 054504.
[125] M. Pérez-Page, V. Pérez-Herranz, *Int. J. Hydrogen Energy* **2014**, *39*, 4009–4015.
[126] G. Wang, W. Zhao, M. Mansoor, Y. Liu, X. Wang, K. Zhang, C. Xiao, Q. Liu, L. Mao, M. Wang, H. Lv, *Nanomaterials* **2023**, *13*, 2818.
[127] Y. Shao, G. Yin, Y. Gao, P. Shi, *J. Electrochem. Soc.* **2006**, *153*, A1093.
[128] N. Giordano, P. L. Antonucci, E. Passalacqua, L. Pino, A. S. Aricò, K. Kinoshita, *Electrochim. Acta* **1991**, *36*, 1931–1935.
[129] L. Castanheira, W. O. Silva, F. H. B. Lima, A. Crisci, L. Dubau, F. Maillard, *ACS Catal.* **2015**, *5*, 2184–2194.
[130] H. Singh, S. Zhuang, B. Ingis, B. B. Nunna, E. S. Lee, *Carbon* **2019**, *151*, 160–174.
[131] T. Lazaridis, H. A. Gasteiger, *J. Electrochem. Soc.* **2021**, *168*, 114517.
[132] J. Wang, S. Wang, *Chem. Eng. J.* **2020**, *401*, DOI 10.1016/j.cej.2020.126158.
[133] F. Haimerl, J. P. Sabawa, T. A. Dao, A. S. Bandarenka, *ChemElectroChem* **2022**, *9*, 1–8.
[134] K. Ehelebe, N. Schmitt, G. Sievers, A. W. Jensen, A. Hrnjić, P. Collantes Jiménez, P. Kaiser, M. Geuß, Y.-P. Ku, P. Jovanovič, K. J. J. Mayrhofer, B. Etzold, N. Hodnik, M. Escudero-Escribano, M. Arenz, S. Cherevko, *ACS Energy Lett.* **2022**, *7*, 816–826.
[135] Q. Meyer, S. Liu, K. Ching, Y. Da Wang, C. Zhao, *J. Power Sources* **2023**, *557*, 232539.
[136] K. J. J. Mayrhofer, D. Strmcnik, B. B. Blizanac, V. Stamenkovic, M. Arenz, N. M. Markovic, *Electrochim. Acta* **2008**, *53*, 3181–3188.
[137] K. Ehelebe, J. Knöppel, M. Bierling, B. Mayerhöfer, T. Böhm, N. Kulyk, S. Thiele, K. J. J. Mayrhofer, S. Cherevko, *Angew. Chem. Int. Ed.* **2021**, *60*, 8882–8888.
[138] P. Lauf, V. Lloret, M. Geuß, C. C. Collados, M. Thommes, K. J. J. Mayrhofer, K. Ehelebe, S. Cherevko, *J. Electrochem. Soc.* **2023**, *170*, 064509.

[139] P. Jovanovič, K. Stojanovski, M. Bele, G. Dražić, G. Koderman Podboršek, L. Suhadolnik, M. Gaberšček, N. Hodnik, *Anal. Chem.* **2019**, *91*, 10353–10356.
[140] A. Hrnjić, F. Ruiz-Zepeda, M. Gaberšček, M. Bele, L. Suhadolnik, N. Hodnik, P. Jovanovič, *J. Electrochem. Soc.* **2020**, *167*, 166501.
[141] S. M. Rezaei Niya, M. Hoorfar, *J. Power Sources* **2013**, *240*, 281–293.
[142] Z. Tang, Q.-A. Huang, Y.-J. Wang, F. Zhang, W. Li, A. Li, L. Zhang, J. Zhang, *J. Power Sources* **2020**, *468*, 228361.
[143] J. Thuriot-Roukos, M. Bennis, E. Heuson, P. Roussel, F. Dumeignil, S. Paul, *RSC Adv.* **2018**, *8*, 40912–40920.
[144] J. Bolze, V. Kogan, D. Beckers, M. Fransen, *Rev. Sci. Instrum.* **2018**, *89*, DOI 10.1063/1.5041949.
[145] I. Martens, A. Vamvakeros, R. Chattot, M. V. Blanco, M. Rasola, J. Pusa, S. D. M. Jacques, D. Bizzotto, D. P. Wilkinson, B. Ruffmann, S. Heidemann, V. Honkimäki, J. Drnec, *J. Power Sources* **2019**, *437*, 226906.
[146] M. A. Isaacs, J. Davies-Jones, P. R. Davies, S. Guan, R. Lee, D. J. Morgan, R. Palgrave, *Mater. Chem. Front.* **2021**, *5*, 7931–7963.
[147] S. Helmly, R. Hiesgen, T. Morawietz, X.-Z. Yuan, H. Wang, K. Andreas Friedrich, *J. Electrochem. Soc.* **2013**, *160*, F687–F697.
[148] E. H. Majlan, D. Rohendi, W. R. W. Daud, T. Husaini, M. A. Haque, *Renewable Sustainable Energy Rev.* **2018**, *89*, 117–134.
[149] S. R. Choi, D. Y. Kim, W. Y. An, S. Choi, K. Park, S.-D. Yim, J.-Y. Park, *Mater. Sci. Energy Technol.* **2022**, *5*, 66–73.
[150] S. Zils, M. Timpel, T. Arlt, A. Wolz, I. Manke, C. Roth, *Fuel Cells* **2010**, *10*, 966–972.
[151] A. P. Soleymani, M. Reid, J. Jankovic, *Adv. Funct. Mater.* **2023**, *33*, DOI 10.1002/adfm.202209733.
[152] K. Yu, J. L. Hart, J. Xie, M. L. Taheri, P. Ferreira, *Nano Energy* **2023**, *111*, 108393.
[153] A. Doerr, *Nat. Methods* **2017**, *14*, 34–34.
[154] R. Girod, T. Lazaridis, H. A. Gasteiger, V. Tileli, *Nat. Catal.* **2023**, *6*, 383–391.
[155] R. Chattot, C. Roiron, K. Kumar, V. Martin, C. A. Campos Roldan, M. Mirolo, I. Martens, L. Castanheira, A. Viola, R. Bacabe, S. Cavaliere, P.-Y. Blanchard, L. Dubau, F. Maillard, J. Drnec, *ACS Catal.* **2022**, *12*, 15675–15685.
[156] H.-J. Lee, M. K. Cho, Y. Y. Jo, K.-S. Lee, H.-J. Kim, E. Cho, S.-K. Kim, D. Henkensmeier, T.-H. Lim, J. H. Jang, *Polym. Degrad. Stab.* **2012**, *97*, 1010–1016.
[157] Y. Matsui, T. Suzuki, P. Deevanhxay, S. Tsushima, S. Hirai, in *ASME 2013 11th Int. Conf. Fuel Cell Sci. Eng. Technol.*, American Society Of Mechanical Engineers, **2013**, pp. 1–5.
[158] M. Fathi Tovini, A. Hartig-Weiß, H. A. Gasteiger, H. A. El-Sayed, *J. Electrochem. Soc.* **2021**, *168*, 014512.
[159] T. Đukić, L. J. Moriau, L. Pavko, M. Kostelec, M. Prokop, F. Ruiz-Zepeda, M. Šala, G. Dražić, M. Gatalo, N. Hodnik, *ACS Catal.* **2022**, *12*, 101–115.
[160] X. Lin, C. M. Zalitis, J. Sharman, A. Kucernak, *ACS Appl. Mater. Interfaces* **2020**, *12*, 47467–47481.
[161] C. M. Zalitis, D. Kramer, A. R. Kucernak, *Phys. Chem. Chem. Phys.* **2013**, *15*, 4329.
[162] M. Hunsom, **2011**, pp. 196–247.
[163] E. Barsoukov, J. R. Macdonald, *Impedance Spectroscopy Theory, Experiment, and Applications, Second Edition*, Wiley Interscience, **2005**.
[164] P. Ren, P. Pei, D. Chen, Y. Li, H. Wang, X. Fu, L. Zhang, M. Wang, X. Song, *Energy Convers. Manage.* **2022**, *258*, 115489.
[165] P. Ren, P. Pei, D. Chen, Y. Li, Z. Wu, L. Zhang, Z. Li, M. Wang, H. Wang, B. Wang, X. Wang, *Appl. Energy* **2022**, *306*, 118068.
[166] T. B. H. Tran, P. Huguet, A. Morin, M. Robitzer, S. Deabate, *Electrochim. Acta* **2021**, *372*, 137904.
[167] S. Deabate, P. Huguet, A. Morin, G. Gebel, Y. Lanteri, Z. Peng, A. -K Sutor, *Fuel Cells* **2014**, *14*, 677–693.
[168] M. N. Islam, A. B. Mansoor Basha, V. O. Kollath, A. P. Soleymani, J. Jankovic, K. Karan, *Nat. Commun.* **2022**, *13*, 6157.
[169] Y.-H. Cho, J. Kim, S. J. Yoo, T.-Y. Jeon, M. Ahn, N. Jung, Y.-H. Cho, J. W. Lim, J. K. Lee, W.-S. Yoon, Y.-E. Sung, *J. Power Sources* **2010**, *195*, 5952–5956.
[170] F. C. Cetinbas, R. K. Ahluwalia, N. Kariuki, V. De Andrade, D. Fongalland, L. Smith, J. Sharman, P. Ferreira, S. Rasouli, D. J. Myers, *J. Power Sources* **2017**, *344*, 62–73.
[171] S. Chevalier, N. Ge, M. G. George, J. Lee, R. Banerjee, H. Liu, P. Shrestha, D. Muirhead, J. Hinebaugh, Y. Tabuchi, T. Kotaka, A. Bazylak, *J. Electrochem. Soc.* **2017**, *164*, F107–F114.
[172] P. Krüger, H. Markötter, J. Haußmann, M. Klages, T. Arlt, J. Banhart, C. Hartnig, I. Manke, J. Scholta, *J. Power Sources* **2011**, *196*, 5250–5255.
[173] Diamond, "About Synchrotrons," (accessed April 30, 2024).
[174] T. E. Miller, V. Davies, J. Li, S. Ghoshal, E. Stavitski, K. Attenkofer, S. Mukerjee, Q. Jia, *J. Electrochem. Soc.* **2018**, *165*, F597–F603.
[175] M. Ronovský, M. Myllymäki, Y. Watier, P. Glatzel, P. Strasser, A. M. Bonastre, J. Drnec, *J. Power Sources* **2024**, *592*, 233906.
[176] G. Gebel, O. Diat, S. Escribano, R. Mosdale, *J. Power Sources* **2008**, *179*, 132–139.
[177] J. Lee, H.-D. Nguyen, S. Escribano, F. Micoud, S. Rosini, A. Tengattini, D. Atkins, G. Gebel, C. Iojoiu, S. Lyonnard, A. Morin, *J. Power Sources* **2021**, *496*, 229836.
[178] P. Boillat, E. H. Lehmann, P. Trtik, M. Cochet, *Curr. Opin. Electrochem.* **2017**, *5*, 3–10.
[179] M. A. van Spronsen, J. W. M. Frenken, I. M. N. Groot, *Nat. Commun.* **2017**, *8*, 429.
[180] L. Pavko, M. Gatalo, T. Đukić, F. Ruiz-Zepeda, A. K. Surca, M. Šala, N. Maselj, P. Jovanovič, M. Bele, M. Finšgar, B. Genorio, N. Hodnik, M. Gaberšček, *Carbon* **2023**, *215*, 118458.
[181] ThermoFisher, "SEM Resolution," (accessed April 30, 2024).
[182] A. G. Star, T. F. Fuller, *J. Electrochem. Soc.* **2017**, *164*, F901–F907.
[183] T. Suzuki, S. Tsushima, S. Hirai, *Int. J. Hydrogen Energy* **2011**, *36*, 12361–12369.
[184] D. Spehner, A. M. Steyer, L. Bertinetti, I. Orlov, L. Benoit, K. Pernet-Gallay, A. Schertel, P. Schultz, *J. Struct. Biol.* **2020**, *211*, 107528.

[185] M. & Associates, "Tech Note: WDS vs EDS," can be found under https://mcswiggen.com/TechNotes/WDSvsEDS.htm, **2024**.
[186] X. Llovet, A. Moy, P. T. Pinard, J. H. Fournelle, *Prog. Mater. Sci.* **2021**, *116*, 100673.
[187] G. I. and Analysis, "Electron probe micro-analyzer (EPMA)," (accessed May 7, 2024).
[188] T. Akita, A. Taniguchi, J. Maekawa, Z. Siroma, K. Tanaka, M. Kohyama, K. Yasuda, *J. Power Sources* **2006**, *159*, 461–467.
[189] P. A. Heizmann, H. Nguyen, M. von Holst, A. Fischbach, M. Kostelec, F. J. Gonzalez Lopez, M. Bele, L. Pavko, T. Đukić, M. Šala, F. Ruiz-Zepeda, C. Klose, M. Gatalo, N. Hodnik, S. Vierrath, M. Breitwieser, *RSC Adv.* **2023**, *13*, 4601–4611.
[190] L. Dubau, L. Castanheira, G. Berthomé, F. Maillard, *Electrochim. Acta* **2013**, *110*, 273–281.
[191] D. A. Cullen, R. Koestner, R. S. Kukreja, Z. Y. Liu, S. Minko, O. Trotsenko, A. Tokarev, L. Guetaz, H. M. Meyer, C. M. Parish, K. L. More, *J. Electrochem. Soc.* **2014**, *161*, F1111–F1117.
[192] A. Kregar, T. Katrašnik, *J. Electrochem. Sci. Eng.* **2023**, *13*, 753–770.
[193] A. Kregar, M. Gatalo, N. Maselj, N. Hodnik, T. Katrašnik, *J. Power Sources* **2021**, *514*, 230542.
[194] P. Frühwirt, A. Kregar, J. T. Törring, T. Katrašnik, G. Gescheidt, *Phys. Chem. Chem. Phys.* **2020**, *22*, 5647–5666.
[195] A. Kravos, A. Kregar, T. Katrašnik, *ECS Meet. Abstr.* **2020**, *MA2020–02*, 2098–2098.
[196] A. Kravos, D. Ritzberger, G. Tavc˘ar, C. Hametner, S. Jakubek, T. Katras˘nik, *J. Power Sources* **2020**, *454*, 227930.
[197] A. Kravos, A. Kregar, Ž. Penga, F. Barbir, T. Katrašnik, *J. Power Sources* **2022**, *541*, 231598.
[198] P. Pei, Z. Zhu, X. Fu, *Energy Convers. Manage.* **2024**, *304*, 118179.
[199] J. Zhang, N. Ramaswamy, B. Lakshmanan, S. P. . Kumaraguru, *Fuel Cell Stack Break-in Procedures and Break-in Conditioning Systems*, **2018**.
[200] M. Zhiani, S. Majidi, M. M. Taghiabadi, *Fuel Cells* **2013**, *13*, 946–955.
[201] E. Balogun, A. O. Barnett, S. Holdcroft, *J. Power Sources* **2020**, *3*, 100012.
[202] T. Selmi, A. Khadhraoui, A. Cherif, *Environ. Sci. Pollut. Res. Int.* **2022**, *29*, 78121–78131.
[203] Z. Qi, A. Kaufman, *J. Power Sources* **2002**, *111*, 181–184.
[204] Z. Qi, A. Kaufman, *J. Power Sources* **2003**, *114*, 21–31.
[205] P. A. Rapaport, A. J. Blowers, J. Leistra, L. Balasubramanian, *Fast MEA Break-in and Voltage Recovery*, **2015**.
[206] J.-C. Shyu, K.-L. Hsueh, F. Tsau, *Energy Convers. Manage.* **2011**, *52*, 3415–3424.
[207] Y. Irmawati, Indriyati, *Energy Procedia* **2015**, *68*, 311–317.
[208] T. Đukić, L. J. Moriau, I. Klofutar, M. Šala, L. Pavko, F. J. González López, F. Ruiz-Zepeda, A. Pavlišič, M. Hotko, M. Gatalo, N. Hodnik, *ACS Catal.* **2024**, *14*, 4303–4317.
[209] J. Schrooten, J. M. Marzullo, M. L. Perry, *Performance Enhancing Break-In Method for a PEM Fuel Cell*, **2005**.
[210] F.-B. Weng, B.-S. Jou, A. Su, S. H. Chan, P.-H. Chi, *J. Power Sources* **2007**, *171*, 179–185.
[211] R. J. Stanis, M.-C. Kuo, A. J. Rickett, J. A. Turner, A. M. Herring, *Electrochim. Acta* **2008**, *53*, 8277–8286.
[212] S. Asghari, A. Mokmeli, M. Samavati, *Int. J. Hydrogen Energy* **2010**, *35*, 9283–9290.
[213] S. Zhang, X.-Z. Yuan, J. N. C. Hin, H. Wang, J. Wu, K. A. Friedrich, M. Schulze, *J. Power Sources* **2010**, *195*, 1142–1148.
[214] T.-F. Yang, L.-W. Hourng, T. L. Yu, P.-H. Chi, A. Su, *J. Power Sources* **2010**, *195*, 7359–7369.
[215] J.-M. Jang, G.-G. Park, Y.-J. Sohn, S.-D. Yim, C.-S. Kim, T.-H. Yang, *J. Electrochem. Sci. Technol.* **2011**, *2*, 131–135.
[216] V. B. Silva, A. Rouboa, *J. Electroanal. Chem.* **2012**, *671*, 58–66.
[217] A. Baricci, M. Bonanomi, H. Yu, L. Guetaz, R. Maric, A. Casalegno, *J. Power Sources* **2018**, *405*, 89–100.
[218] M. Kim, J.-N. Park, H. Kim, S. Song, W.-H. Lee, *J. Power Sources* **2006**, *163*, 93–97.
[219] E. Guilminot, A. Corcella, M. Chatenet, F. Maillard, F. Charlot, G. Berthomé, C. Iojoiu, J.-Y. Sanchez, E. Rossinot, E. Claude, *J. Electrochem. Soc.* **2007**, *154*, B1106.
[220] S. H. Jung, S. L. Kim, M. S. Kim, Y. Park, T. W. Lim, *J. Power Sources* **2007**, *170*, 324–333.
[221] V. A. Sethuraman, J. W. Weidner, A. T. Haug, S. Motupally, L. V. Protsailo, *J. Electrochem. Soc.* **2008**, *155*, B50.
[222] W.-M. Yan, X.-D. Wang, D.-J. Lee, X.-X. Zhang, Y.-F. Guo, A. Su, *Appl. Energy* **2011**, *88*, 392–396.
[223] S. Du, B. Millington, B. G. Pollet, *Int. J. Hydrogen Energy* **2011**, *36*, 4386–4393.
[224] C. Francia, V. S. Ijeri, S. Specchia, P. Spinelli, *J. Power Sources* **2011**, *196*, 1833–1839.
[225] G.-B. Jung, K.-Y. Chuang, T.-C. Jao, C.-C. Yeh, C.-Y. Lin, *Appl. Energy* **2012**, *100*, 81–86.
[226] M. Zhiani, S. Majidi, *Int. J. Hydrogen Energy* **2013**, *38*, 9819–9825.
[227] G. Fu, X. Jiang, M. Gong, Y. Chen, Y. Tang, J. Lin, T. Lu, *Nanoscale* **2014**, *6*, 8226–8234.
[228] J. Park, H. Oh, T. Ha, Y. Il Lee, K. Min, *Appl. Energy* **2015**, *155*, 866–880.
[229] M. Zhiani, I. Mohammadi, S. Majidi, *Int. J. Hydrogen Energy* **2017**, *42*, 4490–4500.
[230] M. M. Taghiabadi, M. Zhiani, V. Silva, *Appl. Energy* **2019**, *242*, 602–611.
[231] J. Song, M. Kim, D. Kim, in *13th IEA Heat Pump Conf.*, 13th IEA Heat Pump Conference, Seoul, **2021**, pp. 1893–1897.
[232] W. Y. Hsu, T. D. Gierke, *Macromolecules* **1982**, *15*, 101–105.
[233] A. T. Haug, R. E. White, J. W. Weidner, W. Huang, S. Shi, T. Stoner, N. Rana, *J. Electrochem. Soc.* **2002**, *149*, A280.
[234] J. Hou, W. Song, H. Yu, Y. Fu, Z. Shao, B. Yi, *J. Power Sources* **2007**, *171*, 610–616.
[235] W. Bi, G. E. Gray, T. F. Fuller, *Electrochem. Solid-State Lett.* **2007**, *10*, B101.
[236] Z. Xie, X. Zhao, M. Adachi, Z. Shi, T. Mashio, A. Ohma, K. Shinohara, S. Holdcroft, T. Navessin, *Energy Environ. Sci.* **2008**, *1*, 184.
[237] J. Shan, X. Yan, X. Sun, Z. Hou, P. Qi, P. Ming, *A Fast Activation Method for a Fuel Cell Stack*, **2010**, Chinese Patent 201010010014.3.

[238] S. Mollá, V. Compañ, E. Gimenez, A. Blazquez, I. Urdanpilleta, *Int. J. Hydrogen Energy* **2011**, *36*, 9886–9895.
[239] J. Hou, *Int. J. Hydrogen Energy* **2011**, *36*, 7199–7206.
[240] C. V. Rao, A. L. M. Reddy, Y. Ishikawa, P. M. Ajayan, *Carbon* **2011**, *49*, 931–936.
[241] F. A. Uribe, T. A. Zawodzinski, *Electrochim. Acta* **2002**, *47*, 3799–3806.
[242] J. Zhang, L. Paine, A. Nayar, R. Makharia, *Methods and Processes to Recover Voltage Loss of Pem Fuel Cell Stack*, US 2011/0195324 A1, U.S. Patent, **2011**.
[243] E. A. Galitskaya, E. V. Gerasimova, Y. A. Dobrovol'skii, G. M. Don, A. S. Afanas'ev, A. V. Levchenko, A. V. Sivak, V. V. Sinitsyn, *Tech. Phys. Lett.* **2018**, *44*, 570–573.
[244] D. Wang, Z. Wang, X. Ding, C. Wu, Z. Liang, L. Wang, *A Method and Device for Activation of Proton Exchange Membrane Fuel Cells*, **2020**, CN Patent 2020108842893.
[245] D. Wang, X. Ding, D. Yang, Z. Liang, L. Wang, *AIP Adv.* **2021**, *11*, DOI 10.1063/5.0046879.
[246] G. Gupta, B. Wu, S. Mylius, G. J. Offer, *Int. J. Hydrogen Energy* **2017**, *42*, 4320–4327.
[247] C. Zhang, H. Liu, T. Zeng, J. Chen, P. Lin, B. Deng, F. Liu, Y. Zheng, *Int. J. Hydrogen Energy* **2021**, *46*, 23489–23497.
[248] Z. Xu, Z. Qi, A. Kaufman, *J. Power Sources* **2006**, *156*, 281–283.
[249] N. Jia, B. Giesecke, *Conditioning Method for Fuel Cells*, US 6,896,982 B2, U.S. Patent, **2005**.
[250] C. He, Z. Qi, A. Kaufman, *Electrochemical Method to Improve the Performance of h/Air Pem Fuel Cells and Direct Methanol Fuel Cells*, US 6,730,424 B1, U.S. Patent, **2004**.
[251] S. Toyota, H. Yoshida, H. Kaji, *Fuel Cell Activation Method*, US 2019/0305347 A1, U.S. Patent, **2019**.
[252] H. Dai, D. Yang, P. Ming, B. Li, C. Zhang, D. Wang, *Cailiao Gongcheng* **2023**, *51*, 20–28.
[253] M. Gerard, J.-P. Poirot-Crouvezier, D. Hissel, M.-C. Pera, *Int. J. Hydrogen Energy* **2010**, *35*, 12295–12307.
[254] H. Su, D. Ye, Y. Cai, W. Guo, *Appl. Energy* **2022**, *323*, 119626.
[255] H. H. Voss, R. H. Barton, M. Sexsmith, M. J. Turchyn, *Conditioning and Maintenance Methods for Fuel Cells*, US 2003/0224227 A1, U.S. Patent, **2003**.
[256] C. Eickes, P. Piela, J. Davey, P. Zelenay, *J. Electrochem. Soc.* **2006**, *153*, A171.
[257] A. Taniguchi, T. Akita, K. Yasuda, Y. Miyazaki, *Int. J. Hydrogen Energy* **2008**, *33*, 2323–2329.
[258] W. R. Baumgartner, P. Parz, S. D. Fraser, E. Wallnöfer, V. Hacker, *J. Power Sources* **2008**, *182*, 413–421.
[259] F. Kagami, N. Matsuoka, R. Shimoi, *Fuel Cell Conditioning System and Related Method*, US 2005/0202293 A1, U.S. Patent, **2005**.
[260] C. Yang, M. Hu, C. Wang, G. Cao, *J. Power Sources* **2012**, *197*, 180–185.
[261] M. Debe, *Final Report - Advanced Cathode Catalysts and Supports for PEM Fuel Cells*, Golden, CO (United States), **2012**.
[262] D. Bezmalinović, J. Radošević, F. Barbir, *Acta Chim. Slov.* **2015**, *62*, 83–7.
[263] J. Y. Park, I. S. Lim, E. J. Choi, Y. H. Lee, M. S. Kim, *Renewable Energy* **2021**, *167*, 162–171.
[264] Z. Xu, Z. Qi, C. He, A. Kaufman, *J. Power Sources* **2006**, *156*, 315–320.
[265] M. Hu, R. Zhao, R. Pan, G. Cao, *Int. J. Hydrogen Energy* **2021**, *46*, 3008–3021.
[266] H. S. Choo, J. H. Lee, H. S. Shin, S. K. Lee, *Pre-Activation Method for Fuel Cell Stack*, US 2014/0045086 A1, U.S. Patent, **2014**.
[267] M. Zhiani, S. Majidi, *Int. J. Hydrogen Energy* **2014**, *39*, 12870–12877.
[268] Z. Xu, Z. Qi, A. Kaufman, *J. Power Sources* **2003**, *115*, 49–53.
[269] K. Palanichamy, A. Prasad, S. Advani, *ECS Meet. Abstr.* **2008**, *MA2008–02*, 1091–1091.
[270] A. Barrio, J. Parrondo, F. Mijangos, J. I. Lombrana, *J. New Mater. Electrochem. Syst.* **2009**, *12*, 87–91.
[271] B. P. Anderson, *Preconditioning Fuel Cell Membrane Electrode Assembles*, US 7,608,118 B2, U.S. Patent, **2009**..
[272] V. B. Silva, A. Rouboa, *Fuel Process. Technol.* **2012**, *103*, 27–33.

Manuscript received: June 30, 2024
Revised manuscript received: August 14, 2024
Version of record online: ■■ ■■, ■■■■

REVIEW

In this review, we explore the process of break-in/conditioning of proton-exchange membrane fuel cells (PEMFCs). First, we acknowledge the key activation and degradation mechanisms that can occur during the break-in phase. Then, we highlight the analytical approaches that can be used to monitor these mechanisms. Finally, we synthesize concepts from various reported methods, explaining how each approach addresses the break-in process and identifies which parameters induce specific key mechanisms.

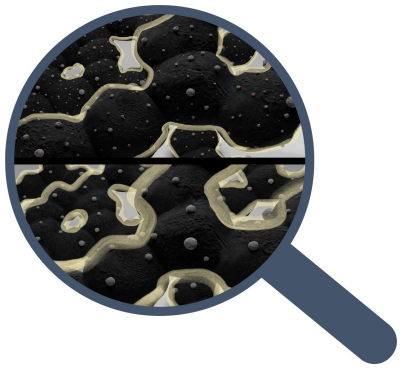

M. Kostelec, M. Gatalo, N. Hodnik**

1 – 31

Fundamental and Practical Aspects of Break-In/Conditioning of Proton Exchange Membrane Fuel Cells